Development of an Adaptive Chemistry Model For Reactive Flow Simulations

by

Ipsita Banerjee

written under the direction of

Dr. Marianthi Ierapetritou

Graduate Program in Chemical and Biochemical Engineering

Rutgers, The State University of New-Jersey

New Brunswick, New Jersey

September, 2003

Abstract

In numerical simulation of combustion models, solution of the chemical kinetics is often the most expensive part of the calculation, since accurate description of kinetic mechanism involves large number of species and reactions, leading to a large set of coupled ODE's, often too complex to be considered in their entirety along with a detailed flow simulation. Hence the need for representing the complex chemical reactions by simple reduced models, which can retain considerable accuracy while rendering computational feasibility. Realistically, under different conditions and at different points in time, different reactions become important, which has been exploited to develop an *adaptive* mechanism reduction scheme such that the reduced reaction model adapts itself to the changing reactor conditions. A methodology is developed in this work to automatically construct reduced mechanisms by utilizing mathematical programming techniques, where the objective is to minimize the dimension of the system while retaining sufficient accuracy in the prediction of species profiles. The reduced kinetic mechanisms are then analyzed for the range of conditions over which they retain their predictive capacity. Those reduced mechanisms are then coupled with the reactive flow algorithm, by selecting the appropriate mechanism depending on reactor condition and integrating the corresponding ODEs for the specified valid range. These ideas are demonstrated using the system of methane combustion in air.

Contents

1 Introduction **1**

2 Mechanism reduction **9**

2.1 Formulation for reaction reduction 9

2.2 Formulation for species reduction 13

2.3 Computationally efficient time stepping reduction 16

2.4 Summary 18

3 Feasibility Analysis of Reduced Mechanism **21**

3.1 Range of Validity of Reduced Mechanisms 21

3.2 Multiperiod Formulation 26

3.3 Feasibility Analysis using Surface Reconstruction 29

3.3.1 α shape approach 29

3.3.2 Selection of α 31

3.4 Feasibility analysis using α shape 34

3.4.1 Sampling technique 35

3.4.2 Range of validity of reduced kinetic model 38

3.5 Summary 41

4 Formulation of Adaptive Reduction **43**

4.1 Stochastic reactor simulation 44

4.1.1 Stochastic simulation of PaSR 44

4.1.2 Stochastic simulation of PMSR 47

4.2 Clustering the accessed space 47

4.3 Generation of library of reduced model 51

4.4 Summary 59

5 Integration with Flow Simulation **60**

5.1 Modeling reactive flows 60

5.2 Riemann Problem 62

5.2.1 Riemann problem for Euler equations 63

5.3 Numerical methods for Euler equations 65

5.3.1 Flux approach 65

5.3.2 Wave approach - Flux vector splitting 65

5.3.3 Wave approach - Reconstruction-Evolution 66

5.3.4 Coflow nonpremixed methane-air flame 70

5.4 Incorporation of adaptive chemistry in flow model 71

5.5 Summary 73

6 Summary and future directions **75**

6.1 Mechanism reduction 75

6.1.1 Application to very large mechanisms 75

6.1.2 Development of reduced models with specific characteristics 76

6.2 Feasibility analysis 78

6.3 Adaptive chemistry scheme 78

6.4 Integration with flow simulation 79

List of Figures

2.1 Performance of species reduction in the prediction of (a) Temperature and (b) CH_4 profiles 15
2.2 Performance of reaction reduction in the prediction of (a) Temperature and (b) CH_4 profiles 15
2.3 Algorithm for adaptive reduction 16
2.4 Adaptively reduced set with $N_{allowable} = 7$ 19
2.5 Comparison of profiles of detailed mechanism and adaptively reduced mechanism 19

3.1 Performance of the reduced mechanism (a) at nominal condition of reduction and (b) at conditions away from the nominal 22
3.2 Performance of α shape for different α values : (a) 120 (b) 200 (c) 100000 . 32
3.3 Performance of α shape with random points 33
3.4 Algorithm of feasibility analysis using α shape 34
3.5 Point-in-polygon test: odd number of intersections means point is inside, even number of intersections means point is outside 35
3.6 Feasible region of a reduced model of GRI-3.0 mechanism involving 17 species and 59 reactions 39
3.7 Predicted feasible region of the reduced model obtained by convex hull approach 39
3.8 Sampled feasible region of a reduced model of GRI-3.0 mechanism 40
3.9 Predicted feasible region of a reduced model 41

4.1 Accessed region for a PaSR (a) projection in Temperature - H_2 plane (b) projection in Temperature - O_2 plane 46

4.2 Accessed region for a PMSR in Temperature - CH_4 - O_2 space 48
4.3 Overall algorithm for adaptive reduction 52
4.4 Range of conditions addressed by different reduced model 52
4.5 Integration with flow simulation 55
4.6 Important reduced models selected at different time intervals 56
4.7 Performance of adaptive reduction in the prediction of (a) temperature and (b) methane profile 57
4.8 Performance of adaptive reduction in the prediction of (a)H and (b) H_2 profile 58

5.1 Performance of reduced mechanism with IEM as micromixing model 64
5.2 Piecewise constant reconstruction of each cell 67
5.3 Each cell edge in a piecewise-constant reconstruction gives rise to a Riemann problem 68
5.4 Projected solution at the next time step 69
5.5 Simulation of Riemann shock tube problem using Godunov scheme 70
5.6 Simulation of Riemann shock tube problem using Godunov scheme, with multiple species 71
5.7 Schematic of the specifications of co-flow methane-air flame 72
5.8 Integration of the adaptive scheme with flow simulation 73

6.1 Sensitivity of laminar flame speed to individual species and reaction 77

List of Tables

3.1 Comparison of the reduced reaction model obtained by using SRSM and multiperiod 28

4.1 Reduced models used for adaptive simulation 53

6.1 Flame speed sensitivity analysis of GRI-3.0 78

Chapter 1

Introduction

Reactive flows can be defined as fluid flows that are significantly affected by chemical reactions, like combustion, dissociation and biochemical processes. Important areas where reactive flows play a vital role include aerospace propulsion, car engine, various manufacturing processes and even biochemical processes like blood circulation. Common to all these examples is the intimate coupling between fluid dynamics and chemistry, which demands a detailed understanding of both processes. The increase in computational capabilities of recent years has contributed significantly towards the goal of accurately simulating reactive flows. This task requires major advances in two areas, computational fluid dynamics (CFD) and physical modeling. Each area is challenging on its own and must be closely coupled to reproduce the physical reality. Using very simple physics (incompressible fluids, or ideal gases) CFD researchers have been able to simulate flow over complicated geometry. On the other hand, by using very simple geometries, many complex physical problems have been investigated. The present challenge, still largely unfulfilled, is to combine geometrical and physical complexity to achieve realistic simulations that can improve the basic understanding of reactive, nonequilibrium fluid flows.

The equations used to model a reactive flow problem are the continuum time- dependent equations for conservation of mass density (ρ), the individual chemical species (y_i), the momentum density (ρv), and the energy density (E). These equations can be written

in a general form as :

$$\frac{\delta \rho}{\delta t} = -\nabla.(\rho v) \tag{1.1}$$

$$\frac{\delta y_i}{\delta t} = -\nabla.(y_i v) - \nabla.(y_i v_{di}) + \dot{\omega}_i, i = 1, \ldots, N_s \tag{1.2}$$

$$\frac{\delta \rho v}{\delta t} = -\nabla.(\rho v v) - \nabla.P \tag{1.3}$$

$$\frac{\delta E}{\delta t} = -\nabla.(Ev) - \nabla.(v.P) - \nabla.(q + q_r) \tag{1.4}$$

The total energy E is defined as:

$$E = 1/2 \rho v.v + \rho \epsilon \tag{1.5}$$

$$\rho \epsilon = \sum_i \rho_i h_i - P \tag{1.6}$$

In addition to the above conservation equations, expressions are required for the thermal and caloric equation of state. For an ideal gas this is given by:

$$P = \rho R T \tag{1.7}$$

$$h_i = H_{i0} + \int_{T^0}^{T} C_{pi} dT \tag{1.8}$$

The terms represented explicitly in equation (1.1 - 1.4) are the convective transport, chemical reactions and physical diffusion, such as thermal conduction and molecular diffusion. Flow simulation in the absence of reaction will involve solution of the set of Navier-Stokes equations, corresponding to mass, momentum and energy balance (Equations 1.1,1.3,1.4). The reactive flow simulation will require in addition to the Navier-Stokes equation, a set of N_s conservation equations, describing the balance of N_s species appearing in the flow.

The reactive flow equations, thus, will require additional modeling to describe the chemical reaction term. In general, one wishes to predict the mass fraction of N_s species which react through N_r chemical reactions. However, the kinetic scheme describing the species as well as reaction for a given situation is not unique. For example, in a hydrocarbon/air flame, N_s may typically change from two to several hundred, while N_r may vary between one and a thousand or more (Williams (1985)), depending on the precision expected from the computation and on the existence of reliable kinetic data. Typically, the chemical source term in Equation (1.2) ($\dot{\omega}_i$) consisting of elementary reversible (or irreversible) reactions involving N_s chemical species can be represented in the general

form :

$$\sum_{k=1}^{N_s} \nu'_{ki}\gamma_k \Leftrightarrow \sum_{k=1}^{N_s} \nu''_{ki}\gamma_k, i = 1, \ldots, N_r \tag{1.9}$$

where ν_{ki} represents the stoichiometric coefficient and γ_k is the chemical symbol for the k_{th} species. The superscript ($'$) indicates forward and ($''$) indicates reverse stoichiometric coefficient. The production rate of the k^{th} species can be written as a summation of the rate of progress for all reactions involving the k^{th} species :

$$\dot{\omega_k} = \sum_{i=1}^{N_r} \nu_{ki} q_i \tag{1.10}$$

$$\nu_{ki} = \nu''_{ki} - \nu'_{ki} \tag{1.11}$$

The rate of progress q_i for the i^{th} reaction is given by the difference of the forward and reverse rates as :

$$q_i = k_{fi} \prod_{k=1}^{N_s} [X_k]^{\nu'_{ki}} - k_{ri} \prod_{k=1}^{N_s} [X_k]^{\nu''_{ki}} \tag{1.12}$$

where $[X_k]$ is the molar concentration of the k^{th} species and k_{fi} and k_{ri} are the forward and reverse rate constants of the i^{th} reaction.

Over the past couple of decades detailed kinetic networks have been developed to model combustion processes. Although kinetic simulations comprising hundred of species and thousand of reactions is not a constraint in homogenous systems, detailed simulation of complex reacting flow systems having strong coupling of heat and mass transfer is still computationally prohibitive. The stiffness of the embedded kinetics often makes the integration of chemical source term the most expensive step. In practice, to alleviate the computational complexity, the reacting flow models use a skeletal kinetic model instead of the detailed mechanism. There has been considerable effort towards reduced representation of detailed kinetic mechanism to alleviate the computational workload, a detailed review of which can be obtained in Tomlin et al. (1997). Most of the techniques are based on the concept of timescale separation. The chemical processes ocurring in a combustion system span a broad range of time scale spreading over many orders of magnitude, from seconds down to nanoseconds. It is this feature that gives rise to the stiffness of the governing equations for the chemical reactions. Yet the fluid mechanics in reactive flows usually occur at a narrower range, on the order of milliseconds to microseconds. There are typically many chemical processes that are much faster than the fluid dynamic processes, so if one is interested in computing behavior on the scale of the fluid mechanics, several

chemical processes will have already self-equilibrated. The time-scale based reduction techniques are all based on decoupling the fast equilibrating chemical processes, either explicitly or implicitly.

The first such technique is the Quasi Steady State Approximation (QSSA), a mathematical technique that originated early in the twentieth century and was formalized for combustion systems by Peters (1988). It involves setting certain species in steady-state and certain reactions in partial equilibrium. A reduced set of global reactions is thus obtained, where the rates of these reactions are given as functions of several rates in the original detailed mechanism. The ODEs for these reduced reaction rates can then be solved in conjunction with algebraic expressions for the concentration of the steady-state species. Typically, partial equilibrium relations are used to simplify these algebraic relations to explicit expressions for efficient solution. QSSA is a relatively simple technique to apply, although it involves considerable *chemist's intuition* to know which species to set in steady-state and which reactions in partial equilibrium. Tools have been developed to aid this process (Turanyi et al., 1996) but they still require a set of appropriate model problems in which to examine the rates. Hence the method has still not been fully automated, and is essentially a hand-powered analytical technique.

A rigorous mathematical formulation for mechanism reduction was initiated by the approach of *lumping* (Wei and Kuo (1969), Kuo and Wei (1969)), in which the chemical species are transformed and lumped into a few dynamically equivalent classes. In this method, a system of linear ordinary differential equations describing the evolution of chemical species :

$$\frac{dC}{dt} = KC \tag{1.13}$$

is transformed into a kinetically equivalent but reduced set of equations :

$$\frac{dc}{dt} = kc \tag{1.14}$$

where, $C = \{C_1, C_2, \ldots, C_n\}^T$ is an n-dimensional column vector of concentrations of all the reacting species in the system and $c = \{c_1, c_2, \ldots, c_m\}^T$ is an m-dimensional column vector of the *lumped* concentration, where m is much smaller than n. The lumped concentrations c are defined as linear combination of the original concentration C.

Frenklach (1984) suggested the *solution mapping* approach, where the model responses are expressed as simple algebraic functions (usually polynomials) in terms of the model

variables. These algebraic functions, called *response surfaces*, are obtained by carrying out several thousands computer simulation using the complete kinetic model. These simulations are performed at preselected combinations of the values of the model variables. If the fitted function has less variables than that of the original mechanism, a reduced dimension model is produced. The repro-modelling approach has been successfully used in atmospheric chemistry and in several areas of combustion chemistry, like in the simulation of hydrocarbon ignition, shock waves, laminar and turbulent flames. These methods are taken from the field of *response surface design* (Box and Draper (1987)), developed for optimization of a poorly understood process by performing the smallest number of experiments possible.

A more recent effort towards automation of mechanism reduction was made in the Intrinsic Low Dimensional Manifold (ILDM method) and Computational Singular Perturbation (CSP) Lam and Goussis (1994) method. They offer considerable advantages over QSSA but are significantly more complicated to implement. The ILDM method (Mass and Pope (1992)) explicitly computes the low dimensional manifolds on which the slow chemistry evolves in the reaction state space, then tabulates the computed results in a lookup table for later use in reactive flow code. The CSP method uses a transformation of the system basis vectors to automatically compute the optimum steady state and partial equilibrium relationship. Unlike ILDM it gives rise to an explicit reduced mechanism, thus providing better understanding of the rate-limiting chemistry.

An alternative to mechanism reduction is the In situ Adaptive Tabulation (ISAT) technique proposed by Pope (1997). The basic idea behind ISAT is to integrate the chemical source term and store the reaction mapping and sensitivity information in a binary tree data structure for later use. For subsequent calculations, for points within a small distance of the previously tabulated points, direct integration is avoided by estimating the reaction mapping using multilinear interpolation. Any reaction mapping that cannot be interpolated with sufficient accuracy is generated by direct integration and stored in a table.

Another suggested approach towards automation of the mechanism reduction is the mathematical programming based approach (Androulakis (2000),Petzold and Zu (1997), Edwards et al. (2000)), which will be adopted in the present work. This approach is based on determining the reactions which can be excluded from the detailed mechanism

while still retaining desired accuracy in the prediction of the profiles of certain important species. This approach renders lot of flexibility in the generation of the reduced model, which can overcome the shortcomings of the previous methods. Following this approach it is possible to generate reduced models possessing specific user defined property and accuracy, which gives the flexibility to generate different reduced models to serve different purposes. Also it gives an estimate of the error incurred by using the reduced model.

In practice, to alleviate the computational complexity, the reacting flow models use a skeletal kinetic model instead of the detailed mechanism, determined by the procedures discussed above. However, for most of the reduction schemes mentioned before, the simplified kinetic model represents the chemical activity tolerably well in a limited region of the flow field and is not accurate over the entire temperature/composition space of interest. In the absence of detailed study of the range of validity of reduced model, the CFD simulation uses the same reduced model over the entire range of conditions, thereby incorporating significant error in the simulation. To overcome these problems an adaptive chemistry approach has been proposed in this work where different chemical behavior of the reactive flow simulations is represented by different reduced models, thereby maintaining sufficient accuracy with significantly reduced models. Though this work concentrates only on combustion systems, but the proposed method is general and can be applied to any reacting system.

In a reactive flow simulation, typically, different regions in the flow field encounter vastly different conditions of species concentration and temperature, which again evolves with time. Hence the nature of chemical reactions going on at different regions at different times are very different. For example, in a flame propagation model, the moving flame front has a strongly exothermic reaction going on, which moves forward with time. The region behind this moving flame front consists of burnt gases at a high temperature but low fuel and oxidiser concentration, while the region ahead of the flame front is rich in fuel and oxidiser, but has insufficient temperature to trigger off combustion. Hence, depending on the involved chemistry, the flow field can be roughly divided into three zones, the location of which again evolves with time. This phenomenon leads to the understanding that different regions of the flow field has entirely different chemistry going on at any instant of time, and the local chemistry in itself is also a function of time. The detailed description of the kinetic network contains information regarding all possible conditions

and is capable of capturing the vastly different kinetic behavior at the diverse conditions encountered. However, when such a detailed network is represented by a reduced set of species and reactions, it is no longer possible to capture the entire domain of behavior with desired accuracy. This means that the reduced representation pertains to a specific region in the flow field and using this model over the entire flow field will lead to erroneous results. This understanding has been exploited in the present work, to develop different reduced schemes to address different regions in the flow simulation, thereby capturing the local behavior with high accuracy, while retaining considerable simplicity in the reduced model.

Chemical kinetics is essentially a local phenomenon, depending only on the conditions of species concentration and temperature. The only effect the flow field has on the local kinetics is the rate at which the flow field changes the species concentration because of diffussion, convection etc., but it directly does not affect the kinetic behavior. Thus, if the CFD code successfully decouples the flow from the kinetics, the kinetic behavior can be adequately expressed as a function of species concentration and temperature. Hence, to start with, what is required is a complete knowledge of the different conditions encountered in the detailed reactive flow simulation. Since solution of the detailed flow model considering an extensive kinetic model is not computationally feasible, an estimate of the accessed composition space has been obtained by solving a homogenous mixing simulation using detailed kinetic model. Different such schemes are evaluated to determine a good estimate of the accessed space. The next step is the generation of a set of reduced reaction models which can address this accessed space. An efficient kinetic mechanism reduction scheme is presented which can reproduce profiles of desired species within user defined accuracy. A formulation is also presented which can restrict the number of reactions in the reduced set by varying the integration time. This enables one to maintain desired simplicity in the reduced model. The next step is determination of the range of conditions over which a particular reduced model can be accurately applied. This is achieved by using the knowledge of feasibility analysis extensively applied in the field of process design. A new approach is presented for efficient approximation of arbitrary shaped feasible region using ideas of surface reconstruction. Feasibility analysis in high dimension is still a field of active research, and conventional techniques for feasibility analysis proves to be computationally infeasible for the present problem. An alternate method for evaluation of

boundary points by reducing the dimension using principal component analysis is found to have satisfactory performance. A multiperiod formulation is also presented in the context of mechanism reduction, which facilitates generation of reduced model possessing a desired flexibility. Having determined the means of generating reduced models and defining the feasible region, the next step towards integration of adaptive reduction with flow simulation is the generation of adequate reduced mechanisms which can cover the accessed region. This requires identification of nominal conditions at which the reduction needs to be performed, which is achieved by clustering the data set and determining representative points for each cluster. An algorithm is presented following which a library of reduced models can be generated, which covers the entire accessed region of the flow simulation. The developed scheme is implemented first in the stochastic reactor model to validate its performance. Finally a detailed reactive flow model is developed for combustion simulation. The adaptive scheme is incorporated in the flow model, where the flow simulation uses reduced kinetic models developed using the data from stochastic reactor model. The performance of the adaptive model is verified using against the detailed model.

The thesis is organized as follows: Chapter 2 presents the methodology for generation of the reduced mechanism, and formulations for restricting the number of reactions in the reduced model. This is followed by the feasibility analysis of the reduced mechanism presented in Chapter 3. Chapter 4 gives the detailed description of the proposed adaptive chemistry scheme, followed by the incorporation of the scheme in a detailed reactive flow model, presented in Chapter 5. A summary of the overall approach and detailed discussion of the areas requiring further attention are presented in Chapter 6.

Chapter 2

Mechanism reduction

Over last couple of decades there has been considerable effort towards development of suitable technique for reduction of complex kinetic mechanism to enable detailed simulation of reactive flow models. The main challenge of this effort is in the development of a completely automated procedure for the generation of reduced models, which can be easily incorporated in the CFD codes. The mathematical programming based approach was found to meet these requirements, and has the additional advantage of generating reduced models tailored to desired mechanism characteristics. Detailed description of the formulation of mechanism reduction problem and the solution technique are presented in this chapter.

2.1 Formulation for reaction reduction

The reduction technique adopted in this work follows the main idea of mathematical programming approach proposed by Androulakis (2000). This approach assumes that the detailed kinetic network of the concerned process is known with considerable accuracy, and it aims at eliminating reactions/ species which are of lower importance in determining the profiles of the desired species. Hence the objective is to minimize the total number of reactions retained in the reduced model, while the constraint is to predict the profiles of the important species with desired accuracy. Such an optimization problem for an

isobaric batch reactor can be formulated as follows :

$$\min_{\lambda \in \Lambda^{N_R}} \sum_{r=1}^{N_R} \lambda_r$$

$$subject\ to\ \chi \leq \delta \tag{2.1}$$

$$where, \chi = \Big(\sum_{k \in \kappa} \int_{t_I}^{t_F} \Big(\frac{y_k^{reduced}(t) - y_k^{full}(t)}{y_k^{full}(t)} \Big)^2 dt + \int_{t_I}^{t_F} \Big(\frac{T_k^{reduced}(t) - T_k^{full}(t)}{T_k^{full}(t)} \Big)^2 dt \Big)^{1/2} \tag{2.2}$$

$$\frac{dy_k(t)}{dt} = \frac{R_k M_k}{\rho} \quad k = 1, ..., N_s \tag{2.3}$$

$$\frac{dT}{dt} = - \sum_{k=1}^{N_s} \frac{R_k M_k h_k}{\rho \overline{C}_p} \tag{2.4}$$

$$R_k = \sum_{i=1}^{N_r} \lambda_i \Big(\nu_{ki}^r - \nu_{ki}^f \Big) q_i \tag{2.5}$$

$$q_i = k_{f_i} \prod_{k=1}^{N_s} X_k^{\nu_{ki}^f} - k_{r_i} \prod_{k=1}^{N_s} X_k^{\nu_{ki}^r} \tag{2.6}$$

$$k_{f_i} = K_{f_i} e^{-E_{f_i}/RT}, k_{r_i} = K_{r_i} e^{-E_{r_i}/RT} \tag{2.7}$$

where, λ_r is a binary variable used to denote the presence ($\lambda_r = 1$) or absence ($\lambda_r = 0$) of a particular reaction. The objective function $\sum_{r=1}^{N_R} \lambda_r$ represents the total number of reactions in the reduced set, which has to be minimized, subject to a specified accuracy (δ). The integral error measure χ, given by Equation (2.2), defines the approximation error of the trajectories of the key observable quantities for the interval of interest. In the above formulation, y_k denotes the mass fraction whereas X_k represents the molar concentration of specie k used in the calculation of the reaction rates. Equations (2.3) and (2.4) represent the material and energy balances for the reactor model, where R_k is the net rate of production of specie k; M_k is the molecular weight of specie k; ρ denotes the mixture density, which is a function of composition and temperature. R_k is evaluated from the knowledge of intrinsic rates q_i of individual reactions and stoichiometry, as given by Equation (2.5). For combustion systems, the basic form of q_i is expressed by the power law expression of mass-action kinetics, as given by Equation (2.6). The temperature dependence of the specific reaction rate constant is given by Arrhenius law (Equation (2.7)).

Formulation (2.1) - (2.7) of mechanism reduction corresponds to an integer nonlinear programming problem which can be solved using a Branch and Bound framework (Androulakis, 2000). The solution procedure can be greatly enhanced by *a priori* determination of a subset of important reactions, thereby reducing the total number of binary variables considered in the Branch and Bound framework. The approach adopted to determine a critical set of reactions ($N_{R^{min}}$) that cannot be removed from the mechanism is as follows: if dropping reaction i from the detailed network ($\lambda_i = 0$) while retaining all other reactions ($\lambda_j = 1, j = 1, \ldots, N_R, j \neq i$) produces a reduced network with $N_r' = N_R - 1$ reactions that approximates the complete network with an error $\delta' > \delta$, then reaction i must be retained in the reduced set and need not be treated as a variable in the optimization problem. Hence, the optimization is now constrained on the remaining $N_R - N_{R^{min}}$ reactions, from which the minimum number of reactions needs to be identified. However, compensating errors can be present, whereby removing reaction A or reaction B can result in an error, but removing reactions A and B together might cancel out individual errors. Such compensating errors cannot be identified by the heuristics. Hence, when such a preprocessing step is employed, the final reduced reaction set obtained might not be optimal.

In the present work, Genetic Algorithm (GA) has been used as the solution procedure for the mechanism reduction problem, following the work of Edwards et al. (1998). GA (Goldberg (1989), Michalewicz and Schoenauer (1996)) represent a class of search and optimization procedures that are patterned after the biological process of natural selection and they lend themselves to solution of a wide range of optimization problems. When GA is applied to optimization problem, each optimization variable is typically encoded as a string of bits, and these strings are appended together to form a chromosome. Each individual in a population has a particular chromosome value that can be decoded to evaluate the parameter values and objective function, also called the fitness function. Populations are evolved through several generations until the objective function cannot be improved any further.

In the present formulation the optimization variables are the N_R binary variables associated with the reactions. Hence parameterisation for GA is straightforward since each binary variable λ_r becomes a bit in the GA chromosome. For a particular combination of λ_r the reduced differential equation sets are integrated to evaluate the discrepancy func-

tion. Since GA cannot explicitly handle nonlinear constraints of an optimization problem, there has been considerable research towards efficient constraint handling while using GA. Most of the constraint handling methods are based on the concept of (exterior) penalty functions (Michalewicz and Schoenauer, 1996) that penalize the infeasible solution and try to solve an unconstrained problem using a modified fitness function. The unconstrained optimization for problem (2.1) - (2.7) can be formulated as:

$$\min_{\lambda \in \Lambda^{N_R}} \sum_{r=1}^{N_R} \lambda_r + (penalty \times max\{0, \chi - \delta\}) \tag{2.8}$$

where the penalty term becomes zero when the constraint is not violated ($\chi < \delta$), and it takes the value of a large positive quantity ($penalty \times (\chi - \delta)$) otherwise. Note that the penalty coefficient needs to be large enough to ensure that all the infeasible solutions have fitness value worse than any of the feasible solutions. Unlike classical search and optimization methods, GA approach begins its search with a random set of solutions, instead of just one solution.

For the solution of problem (2.1) - (2.7), the first step of the GA procedure involves the random generation of a large population of binary strings (reaction combinations) where each member of the population represents a reduced reaction set. For each reduced set within the initial population the corresponding ODEs are integrated to evaluate the discrepancy function and hence the fitness function, as given in Equation (2.8). The integration is performed using LSODE (Hindmarsh, 1983) while the rate expressions and all the necessary thermodynamic properties are evaluated using the CHEMKIN-III package (Kee et al., 1996). The generated population of solutions are modified by the GA operators (reproduction, crossover, mutation) to create new and better populations. This procedure is repeated until a predefined termination criteria is satisfied. There are several advantages of using GA for the mechanism reduction problem as compared to Branch and Bound procedure. First, the computation time of Branch and Bound depends highly on the quality of the initial reaction set produced within the preprocessing heuristic step, since the closer it is to the optimal solution the less number of nodes are required. However, as mentioned before, the method of generating the initial guess can prevent optimality of the solution. Since GA does not require such a reaction subset to start the solution procedure, this problem is avoided. Second, in the Branch and Bound procedure, at each node

of the binary tree a nonlinear optimization problem needs to be solved, which requires information of the gradient of the constraint function, that corresponds to an expensive computational step. Moreover, since the NLP is in general nonconvex, no guarantee of the global optimal solution is possible. GA does not require gradient evaluation since the only information needed is the value of the discrepancy function for certain combinations of reaction sets. On the other hand however, the optimal solution obtained by using GA depends heavily on the termination criteria that are predetermined by the user, which can be a limitation. For the present studies, the simulation was allowed to run sufficient number of times until no significant change in the objective function was observed, which is however not sufficient to guarantee optimality of the obtained solution. GA is adopted in this work for the additional reason that the target is to generate a number of reduced kinetic networks that will be used within the adaptive chemistry framework (Section 5), and not the determination of a single optimal reduced network.

2.2 Formulation for species reduction

The above formulation minimizes the total number of reactions involved in the kinetic source term, and the number of binary variables equals the total number of reactions. For a typical combustion system,the number of reactions far exceeds the total number of species. For example, methane combustion following GRI-3.0 mechanism involves 53 species and 325 reactions. For such a system a preprocessing step of species reduction was observed to be more efficient in solving the optimization problem. Moreover, reducing the number of species is of primary importance, since it directly reduces the number ODE's required to model the kinetic term. However, all the reactions in which the species participates need not be important. Hence a second step of reaction reduction is performed on the retained set, using the formulation consisting of Equations (2.1 - 2.7). The formulation of species reduction is given be:

$$\min_{\lambda \in \Lambda^{N_s}} \sum_{i=1}^{N_s} \lambda_s$$

$$subject\ to\ \chi \leq \delta$$

$$\chi = \Big(\sum_{k \in \kappa} \int_{t_I}^{t_F} \Big(\frac{y_k^{reduced}(t) - y_k^{full}(t)}{y_k^{full}(t)} \Big)^2 dt + \int_{t_I}^{t_F} \Big(\frac{T_k^{reduced}(t) - T_k^{full}(t)}{T_k^{full}(t)} \Big)^2 dt \Big)^{1/2}$$

$$\frac{dy_k(t)}{dt} = \frac{R_k M_k}{\rho} \quad k = 1, ..., N_s$$

$$\frac{dT}{dt} = - \sum_{k=1}^{N_s} \frac{R_k M_k h_k}{\rho \overline{C}_p}$$

$$R_k = \sum_{i=1}^{N_r} \prod_{s=1}^{N_s} (\lambda_s)_r \Big(\nu_{k_i}^r - \nu_{k_i}^f \Big) q_i \tag{2.9}$$

where λ_s is a binary variable corresponding to each specie which determines if specie (s) is present in the network. If a particular specie can be neglected, then the corresponding $\lambda_s = 0$ and all the reactions which involve that specie will be set to 0. However, all the reactions in which the specie participates need not be important. Hence a second step of reaction reduction is performed on the retained set, using the formulation (2.1) - (2.7).

Following this procedure, mechanism reduction was performed for the methane combustion system, with the detailed mechanism described by GRI-3.0 consisting of 53 species and 325 reactions. The initial conditions at which reduction was performed is : H_2 mass fraction of 2.92056×10^{-05}, O_2 mass fraction of 0.468255, CH_4 mass fraction of 0.290531 and temperature of 1208.64 K. The species reduction with an allowable error of 0.1 resulted in a reduced set consisting on 21 species and 99 reactions. Figure (2.1) illustrates the performance of the reduced set in predicting the temperature and CH_4 profiles. The reaction reduction is then performed over this reduced set with the same allowable error, which resulted in the final reduced set consisting of 17 species and 29 reactions. Figure (2.2) illustrates the temperature and CH_4 profiles predicted by this final reduced set.

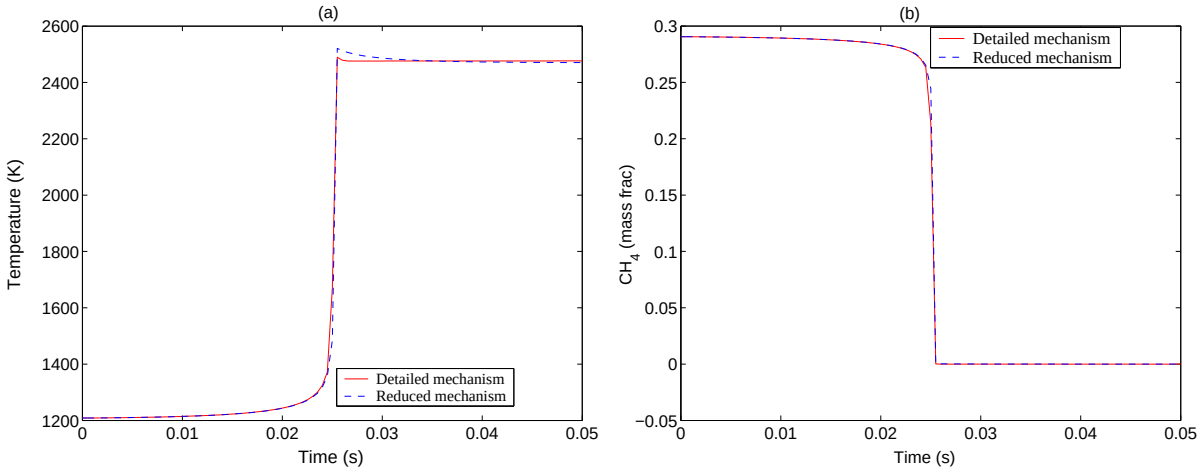

Figure 2.1: Performance of species reduction in the prediction of (a) Temperature and (b) CH_4 profiles

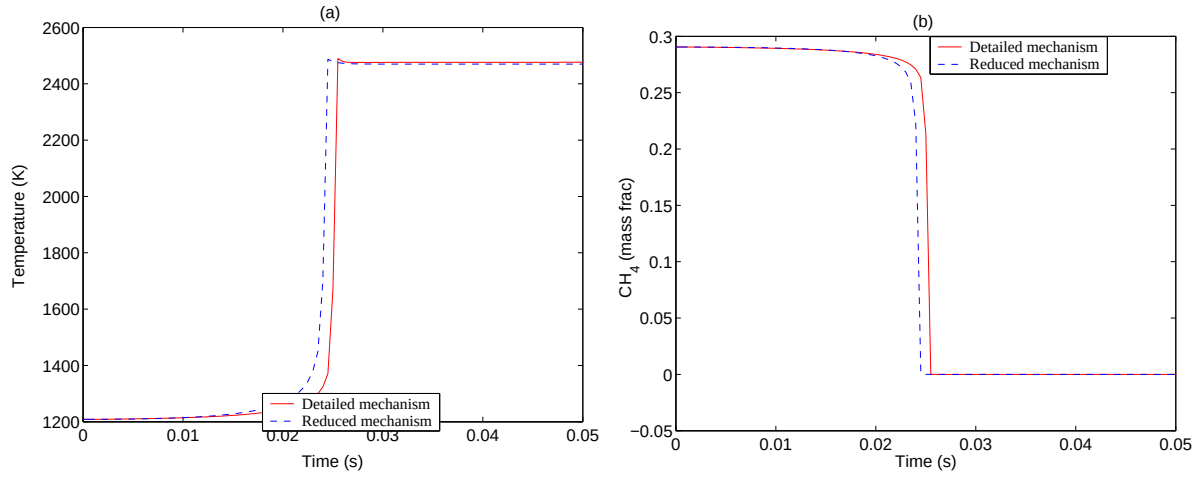

Figure 2.2: Performance of reaction reduction in the prediction of (a) Temperature and (b) CH_4 profiles

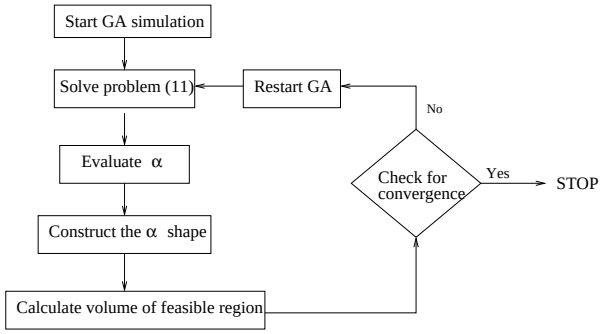

Figure 2.3: Algorithm for adaptive reduction

2.3 Computationally efficient time stepping reduction

Following the procedure mentioned above, it is possible to generate a reduced mechanism at a particular condition which can predict the profiles of the watched species within user defined accuracy. However, such a reduced model can end up being too large for efficient implementation in the complex flow models, since there is no restriction imposed on the size of the reduced reaction set. The procedure is extended here so as to simplify the reduced model without sacrificing accuracy. This is achieved by restricting the integration time over which the reduced model needs to predict the species profiles.

The overall proposed approach of adaptive reduction consists of two steps as illustrated graphically in Figure (2.3). In the first step the entire integration time is uniformly divided into certain number of intervals and a reduced reaction set is obtained for each of the interval through the solution of problem (2.1) - (2.7). In the second step, these intervals are systematically refined to restrict the number of reactions in each of the reduced sets within a prescribed number. The optimization problem solved in the first step of the

approach for each time interval is formulated as :

$$\begin{aligned} &\min_{\lambda \in \Lambda^{N_R}} \sum_{r=1}^{N_R} \lambda_r \\ &subject\ \ to\ \ \chi \leq \frac{\delta}{N_{int}} \\ \chi = \Big(\sum_{k \in \kappa} \int_{t_i^{N_{int}}}^{t_f^{N_{int}}} &\Big(\frac{y_k^{reduced}(t) - y_k^{full}(t)}{y_k^{full}(t)} \Big)^2 dt \\ + \int_{t_i^{N_{int}}}^{t_f^{N_{int}}} &\Big(\frac{T_k^{reduced}(t) - T_k^{full}(t)}{T_k^{full}(t)} \Big)^2 dt \Big)^{1/2} \end{aligned} \tag{2.10}$$

where y_k, T_k are obtained by reactor equations (2.3) - (2.7); N_{int} is user defined number of intervals into which the integration time was divided; $t_i^{N_{int}}$ and $t_f^{N_{int}}$ are the initial and final times for an interval respectively, defining the range over which the differential equations needs to be integrated. To perform the reduction at each interval, the initial conditions for integration is set to the corresponding PSR conditions at that instant. The allowable error was also uniformly divided over each interval. It is observed that when the time domain is divided uniformly, a large number of reactions are retained in the reduced set for the initial stiff portion of the profile. However, after certain time the number of reactions retained in the reduced sets are consistently low. The intervals containing unacceptably high number of reactions are identified and considered at the second step of the procedure for further refinement. The purpose of the second step is to identify the reduced set with acceptable number of reactions, and also determine the time over which the reduced set can be integrated to attain the prescribed accuracy. This is achieved by solving the following optimization problem :

$$\begin{aligned} &\max t_f \\ &subject\ \ to\ \ \sum_{r=1}^{N_R} \lambda_r < N_{allowable} \\ &\chi \leq \delta^{int}(t) \\ \chi = \Big(\sum_{k \in \kappa} \int_{t_i}^{t_f} &\Big(\frac{y_k^{reduced}(t) - y_k^{full}(t)}{y_k^{full}(t)} \Big)^2 dt \\ + \int_{t_i}^{t_f} &\Big(\frac{T_k^{reduced}(t) - T_k^{full}(t)}{T_k^{full}(t)} \Big)^2 dt \Big)^{1/2} \end{aligned} \tag{2.11}$$

where y_k, T_k are obtained by the reactor equations (2.3) - (2.7); $N_{allowable}$ represents the

maximum allowable size of the reduced set, which is user defined depending on number of reactions which can be handled by the CFD code; t_f represents the time over which the differential equations for reduced reaction set can be integrated while still retaining the desired accuracy of the species profiles. This optimization problem is solved using Genetic Algorithm, where both reaction time and λ_r are treated as variables. With this formulation, the aim is to obtain various reduced sets of $N_{allowable}$ reactions or less, along with the integration time over which the particular set is valid. To maintain a desired accuracy over the entire integration time, the allowable error is expressed as a linear function of time. Hence if an error of δ is allowed between t_F and t_I, for each optimization subproblem the allowable error is expressed as:

$$\delta^{int}(t) = \frac{\delta}{(t_F - t_I)}(t_f - t_i) \tag{2.12}$$

where t_i and t_f are the initial and final time for the current iteration. Problem(2.11) is solved in an iterative manner, starting with an initial time ($t_i^{N_{int}}$) identified from the first step of the algorithm, and marching forward towards the final time ($t_f^{N_{int}}$) of that particular interval. At each iteration, the ODEs representing the reactor behavior is integrated from an initial time t_i which corresponds to the optimum time of the previous iteration. The current integration is performed until t_f which is an optimization variable. This reduction scheme was performed for the kinetic scheme of CO/H_2 combustion in air, consisting of 47 reactions and 14 species. The initial conditions considered are: H_2 mole fraction = 0.005, O_2 mole fraction = 0.189, CO mole fraction = 0.095, N_2 mole fraction = 0.711, T_0 = 1600K. The reduced reaction sets obtained by fixing $N_{allowable} = 7$ is illustrated in Figure (2.4), and the performance of these reduced sets in the prediction of temperature and H_2 profiles in a perfectly stirred reactor is illustrated in Figure (2.5).

2.4 Summary

A detailed formulation of the mechanism reduction scheme was presented in this chapter, which allows automatic generation of reduced kinetic models. The scheme was used to reduce methane/air combustion system, where a two step procedure of species reduction followed by reaction reduction was found to be of particular advantage. The presented scheme could significantly reduced the dimension of the mechanism while retaining consid-

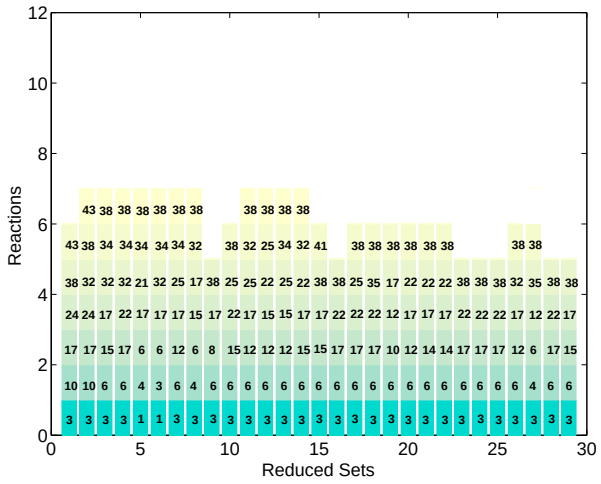

Figure 2.4: Adaptively reduced set with $N_{allowable} = 7$

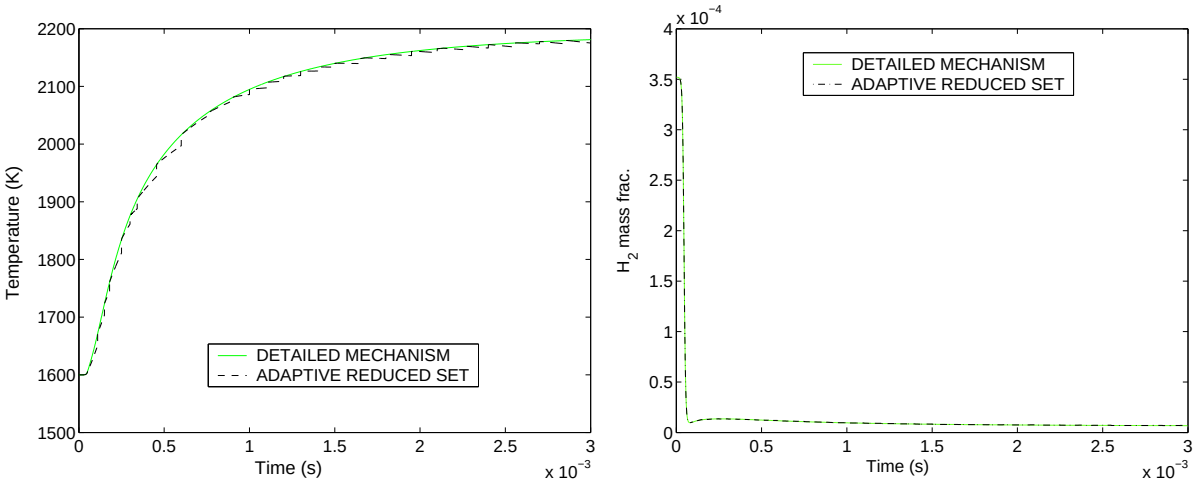

Figure 2.5: Comparison of profiles of detailed mechanism and adaptively reduced mechanism

erable accuracy in the prediction of species profiles. A scheme for restricting the number of reactions in the reduced mechanism is also presented and was tested for CO/air mechanism.

Chapter 3

Feasibility Analysis of Reduced Mechanism

The reduced mechanism obtained by the procedure mentioned in the previous chapter maintains its accuracy over a restricted range of species concentration and temperature. Since using a reduced mechanism in a region where it is not valid will introduce significant error, it is imperative to have an accurate description of the feasible region of operation. Existing techniques of feasiblity analysis has the disadvantage of underestimating the feasible region. Moreover, the required number of simulations is prohibitively high in systems of higher dimensions. An alternative method of feasibility analysis for mechanism reduction problem is presented here, which overcomes the problems of existing techniques.

3.1 Range of Validity of Reduced Mechanisms

A single reduced mechanism has the property of predicting the profiles of the observed species within certain user defined accuracy at the initial condition of species concentration and temperature at which the reduction was performed. While this reduced model can accurately predict the system performance over a certain region in and around the nominal condition of reduction, but if integrated at entirely different conditions, there is no guarantee on the accuracy of prediction of the reduced model. This is illustrated in Figure (3.1), where in plot (a) the integration was performed under the same condition at which the reduction was performed, namely H_2 mass fraction $= 2.92056 \times 10^{-5}$, O_2

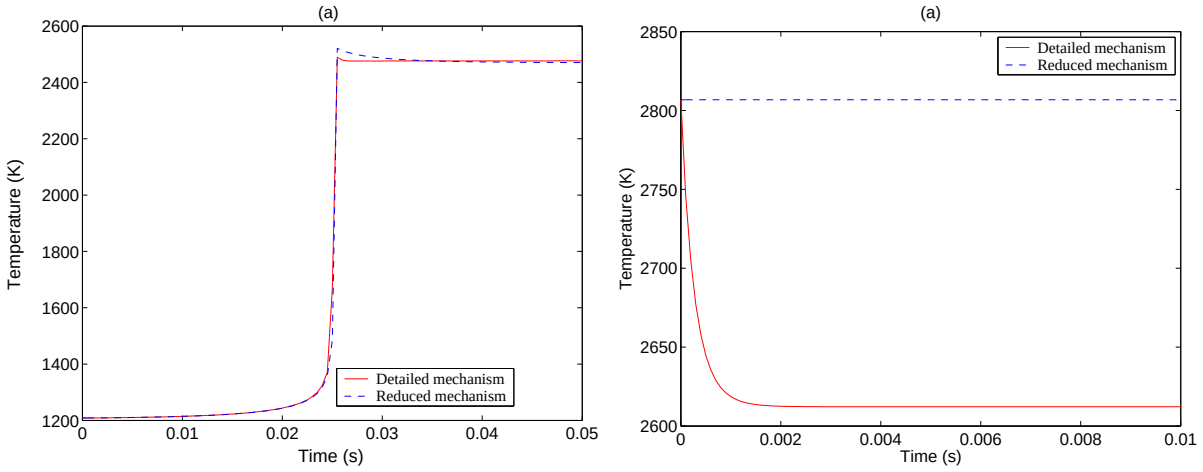

Figure 3.1: Performance of the reduced mechanism (a) at nominal condition of reduction and (b) at conditions away from the nominal

mass fraction = 0.468255, CH_4 mass fraction = 0.290531 and T = 1208.64 K, and in plot (b) the integration was performed at a different condition of H_2 mass fraction = 9.35160×10^{-2}, O_2 mass fraction = 1.28092×10^{-12}, CH_4 mass frac = 1.13365×10^{-4} and T = 2806.78 K. It is observed that although the reduced model predicts the temperature profile at the nominal condition with great accuracy, at conditions away from the nominal its performance deteriorates significantly. Hence it is neccessary to quantify the range of species concentration at which the reduced model can predict the species profiles within user defined accuracy. This leads to the problem of feasibility analysis, formulated by Swaney and Grossmann (1985) , (1985b). The idea of feasibility/flexibility analysis was developed in the context of chemical process design and operation, where an important problem is to maintain feasible steady state operation for a range of uncertain conditions that may be encountered during a plant operation. Thus the design flexibility can be defined as the ability of a design to tolerate and adjust to variations in parameter conditions which may be encountered during operation. Thus the problem of optimal flexible design consists of (a) determination of a process configuration at a chosen nominal point and (b) determination of the range of process parameters the optimal configuration can tolerate.

The present problem of kinetic model reduction can be considered, following the same ideas as for the process synthesis problem, wherein the problem of determining an optimal reduced model at a nominal point is identical to step (a), and determining the range of

species concentration over which the reduced model is valid is similar to step (b). Hence the techniques of flexibility analysis used for process design problems can be applied in the present problem of mechanism reduction, as was successfully demonstrated by Sirdeshpande et al. (2001).

Following the idea of Halemane and Grossmann (1983), for given nominal conditions θ_i^N, if $\Delta\theta_i^+$ and $\Delta\theta_i^-$ are the maximum expected deviations of the parameters from the nominal point, the expected range of each parameter is :

$$\theta_i^N - \Delta\theta_i^- \leq \theta_i \leq \theta_i^N + \Delta\theta_i^+ \tag{3.1}$$

To determine the flexibility of a mechanism, a new parameter σ is introduced, using which the expected parameter range can be expressed as :

$$\theta_i^N - \sigma\Delta\theta_i^- \leq \theta_i \leq \theta_i^N + \sigma\Delta\theta_i^+ \tag{3.2}$$

The aim of flexibility analysis is the determination of the optimal value of σ for which the reduced mechanism predicts the profiles within user defined accuracy. One way of determining this is by the vertex enumeration strategy (VES), where an optimization problem needs to be solved at each vertex of the expected parameter range. The coordinates of the vertices (V^k) for a two-parameter problem are :

$$V^1 = \{\theta_1 + \sigma\Delta\theta_1^+, \theta_2 + \sigma\Delta\theta_2^+\} \tag{3.3}$$

$$V^2 = \{\theta_1 + \sigma\Delta\theta_1^+, \theta_2 - \sigma\Delta\theta_2^+\} \tag{3.4}$$

$$V^3 = \{\theta_1 - \sigma\Delta\theta_1^+, \theta_2 - \sigma\Delta\theta_2^+\} \tag{3.5}$$

$$V^4 = \{\theta_1 - \sigma\Delta\theta_1^+, \theta_2 + \sigma\Delta\theta_2^+\} \tag{3.6}$$

$$\tag{3.7}$$

At each vertex, the following optimization problem is solved :

$$\begin{aligned} &max\ \ \sigma \\ subject\ \ to\ \ &\chi(\theta_1(\sigma), \theta_2(\sigma), \ldots,) \leq 0 \end{aligned} \tag{3.8}$$

The flexibility index is taken to be the smallest value among all the optima obtained from the solution of the optimization problem at all vertices. The VES assumes that the point of constraint violation occurs at one of the vertices of the expected parameter

range. Physically, this method inscribes the largest hyperrectangle within the range of operation, being centered at the nominal point and its sides are proportional to the expected deviations, $\Delta\theta^+, \Delta\theta^-$. Although this approach succeeds in quantifying the feasible region, it can lead to large underestimation of the region, particularly if the nominal point is located close to one of the constraints. Sirdeshpande et al. (2001) proposed estimation of the feasible region by inscribing a convex hull using the boundary points evaluated by solving a number of the optimization problems. A convex hull of a set of points is the smallest convex set that contains all the points. There exists a number of different algorithms in the computational geometry literature that are designed to compute the convex hull for a given set of points. A review can be found in Berg et al. (1997). Recent work on convex hull has been focussed on variations of a randomized, incremental algorithm where points are considered one at a time. *Quickhull algorithm* (Barber et al. (1996)), is such an approach which proceeds using two geometric operations : oriented hyperplane through (n_d) points and signed distance to hyperplane. In particular, the following steps are followed for each processed point :

1. Locate the visible facets for the point. A facet is visible if the point is above the facet. The selection is made by evaluating the signed distance from the facet.

2. Construct a cone of new facets from the point to the visible facets.

3. Delete the visible facets thus forming the convex hull of the new point and the previous processed points.

Following the above procedure, determination of the feasible region of an n parameter problem would require solution of 2^n optimization problems, which is impractical for high values of n. This is of particular concern for the applicability of this procedure in the problem of mechanism reduction, since the dimension of the kinetic problem is expected to be of the order of the number of species present in the system, and the evaluation of the constraint function is also expensive. An alternative approach for determining the boundary points of the feasible region of a reduced mechanism is to start from the nominal point and proceed along the direction where the error constraint is most sensitive to changes in the initial conditions. Such directions can be determined by performing a sensitivity analysis of the error constraint with respect to initial conditions, followed by the principal

component analysis of the sensitivity matrix. The use of principal directions facilitates the possibility of reduction of dimension by selecting only the significant directions.

Thus the boundary points are determined by solving the following problem :

$$max\sigma$$
$$subject\ to\ \chi(y_1(\sigma), y_2(\sigma), ..., T(\sigma)) \leq 0 \tag{3.9}$$

where σ is a scaled deviation of parameters $y_1, y_2, ..., T$ along the principal direction of the deviation error, defined as :

$$Q(\alpha) = \sum_{j=1}^{q} \sum_{i=1}^{m} \left[\frac{\xi_{i,j}(\boldsymbol{\alpha}) - \xi_{i,j}(\boldsymbol{\alpha}^0)}{\xi_{i,j}(\boldsymbol{\alpha}^0)} \right]^2 \tag{3.10}$$

where $\xi_{i,j}(\boldsymbol{\alpha}) = \xi_i(t_j, \boldsymbol{\alpha})$ denotes the error between detailed and reduced mechanism at each selected time point $(t_j, j = 1, 2, \ldots, q)$ and for each of the m *observed* species. $\boldsymbol{\alpha}$ is a measure of initial species concentration y_i, given as:

$$\alpha_i = \ln y_i, i = 1, 2, \ldots, p \tag{3.11}$$

$\xi_{i,j}(\boldsymbol{\alpha})$ can be seen as the deviation of the reduced profile from the detailed profile under particle conditions, and $\xi_{i,j}(\boldsymbol{\alpha}^0)$ is the same deviation under the nominal condition at which reduction is performed. The classical Gauss approximation gives (Vajda et al. (1985)):

$$Q(\boldsymbol{\alpha}) \approx \tilde{Q}(\boldsymbol{\alpha}) = (\Delta\boldsymbol{\alpha})^T S^T S(\Delta\boldsymbol{\alpha})$$
$$\Delta\alpha_i = \alpha_i - \alpha_i^0 \tag{3.12}$$

where $\Delta\alpha_i$ is the deviation of the particle condition from the nominal condition of reduction. S is the array of normalized sensitivities at each time points $t_1, t_2, \ldots, t_q$, given as:

$$\mathbf{S} = \begin{bmatrix} S_1 \\ S_2 \\ \vdots \\ S_q \end{bmatrix}$$

$$\mathbf{S}_i = \begin{bmatrix} \frac{\partial \ln \xi_{1,i}}{\partial \ln \alpha_1} \frac{\partial \ln \xi_{1,i}}{\partial \ln \alpha_2} \cdots \frac{\partial \ln \xi_{1,i}}{\partial \ln \alpha_p} \\ \frac{\partial \ln \xi_{2,i}}{\partial \ln \alpha_1} \frac{\partial \ln \xi_{2,i}}{\partial \ln \alpha_2} \cdots \frac{\partial \ln \xi_{2,i}}{\partial \ln \alpha_p} \\ \vdots \\ \frac{\partial \ln \xi_{m,i}}{\partial \ln \alpha_1} \frac{\partial \ln \xi_{m,i}}{\partial \ln \alpha_2} \cdots \frac{\partial \ln \xi_{m,i}}{\partial \ln \alpha_p} \end{bmatrix}$$

The principal directions can be obtained by performing singular value decomposition of $S^T S$ expressed as:

$$S^T S = U^T \Lambda U \tag{3.13}$$

where Λ is a diagonal matrix formed by the eigenvalues λ_i of $S^T S$ and U denotes the matrix of orthonormal eigenvectors $u_i, i = 1, 2, \ldots, p$. Bard (1974) defined the principal components as:

$$\Psi = U^T \boldsymbol{\alpha} \tag{3.14}$$

Solving the optimization problem along each of the principal directions leads to the determination of boundary points, which are used to define the approximation of the convex hull of the region of validity. Note that by utilizing the principal component analysis the dimension of the problem can be greatly reduced, thus allowing for more efficient representation of the feasible region. Hence this analysis can be used to identify the dominant variables in the kinetic network reduction problem, thereby making the described feasibility analysis technique applicable to this problem.

3.2 Multiperiod Formulation

The problem discussed in the previous section is primarily to analyzes the performance of a reduced mechanism under variable parameter conditions, which is essentially a post processing step. Hence the problem of mechanism reduction contains no information regarding the range of validity of a particular reduced mechanism. Hence it is possible that a reduced mechanism which is optimal at the nominal point retains its optimality over a very narrow parameter range. This can be avoided by including the effects of parameter uncertainty in the reduction stage, with the aim of determining a reduced model which retains prescribed flexibility. A method to address this issue in design under uncertainty problem is the multiperiod formulation, proposed by Halemane and Grossmann (1983).

For the case of mechanism reduction, it amounts to the determination of an optimal reduced kinetic model, which retains its accuracy over a desired range of initial conditions of species concentrations and temperature. Sirdeshpande et al. (2001) illustrated the performance of this procedure in a H_2/O_2 combustion system. The idea is to generate a population comprised of N_p vectors of uncertain parameters, using a sampling technique. Each member k of the population is known as a scenario, and is represented by the parameter vector θ^k. The optimization problem is formulated as :

$$\begin{aligned} & \min_{\lambda} \sum_{i=1}^{n_r} \lambda_i \\ subject\ to \quad & \chi_k(\lambda; \theta^k) \leq \epsilon, k = 1, \ldots, N_p \end{aligned} \tag{3.15}$$

This problem is similar to problem (2.1) - (2.7), except that the number of error constraints to be satisfied is N_p instead of one, thus making it more computationally intensive. Having obtained an optimal solution, the feasibility problem is solved to verify if the reduced set covers the desired range of conditions. If not, a critical point, from the the set of scenarios considered, is added to the population and the procedure is repeated by solving problem (3.15) with a larger population.

This technique was further tested considering uncertainty in the values of reaction rate constants. This problem becomes particularly important for the suggested reduction scheme since it is entirely based on the availability of a detailed kinetic model consisting of deterministic reaction rate constants. However, such kinetic parameters are experimentally determined and is expected to be uncertain. An optimal reduced model which remains accurate over the uncertain range of kinetic parameter can be determined by solving problem (3.15), wherein the scenario θ^k corresponds to a set of rate constants. The determination of the optimal reduced set is followed by the feasibility analysis of the reduced set, formulated as :

$$\begin{aligned} & \max_{\theta^{K_p}} \chi \\ subject\ to\ & k_{f,i}^{LB} \leq k_{f,i} \leq k_{f,i}^{UB}, i = 1, \ldots, N_R \end{aligned} \tag{3.16}$$

The upper and lower bounds on the reaction rate constants are computed through the uncertainty factors $k_{f,i}^{LB} = k_{f,i}^{nom}/UF_i$ and $k_{f,i}^{UB} = k_{f,i}^{nom} \times UF_i$, where $k_{f,i}^{nom}$ represents the nominal value of the rate constant. Finding a value of $\chi > \epsilon$ indicates that the mechanism

System	SRSM	multiperiod
H_2/O_2	2-8,14	2-8
$H_2/CO/Air$	1,4,6,10,12-15,17	1-4,6,10,12-15,
	17,22,25,35,37,38,43	17,22,24,25,32-35

Table 3.1: Comparison of the reduced reaction model obtained by using SRSM and multiperiod

does not have the desired flexibility and the optimal θ^k values resulting from the solution of problem (3.16) are introduced as a new scenario for problem (3.15). This generates a new mechanism which is again checked for feasibility, and this procedure is repeated until $\chi \leq \epsilon$. This procedure was performed in both H_2/O_2 system and $H_2/CO/Air$ system, and was compared with similar simulation performed with the stochastic response surface (SRSM) based method (Balakrishnan et al. (2002)). The SRSM belongs to the family of surface-response methods where the system outputs are expressed as polynomial functions of the uncertain parameters. The polynomial expansion coefficients are used to extract sensitivity information from the reaction mechanism, which provides a direct measure of the effect of changes in a rate constant on the output concentration of species. This sensitivity information was used to determine the reduced set of reactions and is compared with the reduced mechanism obtained from the multiperiod formulation in Table (3.1).

The feasibility analysis approach presented in section (2.1) performs well for well defined, convex functions. However, the present problem of feasibility analysis of reduced mechanism gives rise to non-convex, even disjoint feasible region, the approximation of which becomes extremely difficult with analytical techniques. The conventional feasibility analysis technique, though applicable in the mechanism reduction problem, largely underestimates the feasible region, thus making its application inefficient. Use of multiperiod formulation can increase the actual feasible region, by incorporating feasibility information in the mechanism reduction stage. However, it does not solve the problem of inefficient approximation of the feasible region. Moreover, it increases the size of the reduced mechanism by forcing it to be feasible over a larger region in the composition space.

3.3 Feasibility Analysis using Surface Reconstruction

A new approach is developed in this work for efficient approximation of arbitrary shaped feasible region using the ideas of shape reconstruction practiced in the field of computer graphics. The main problem definition for surface reconstruction is that given a set of range points, reconstruct a manifold that closely approximates the surface of the original model. Range data is a set of discrete points in three dimensional space which have been sampled from the physical environment or can be obtained using laser scanners which generate data points on the surface of an object. The problem naturally arises in a variety of practical situations such as range scanning an object from multiple view points, recovery of biological shapes from two-dimensional slices, interactive surface sketching etc. Surface reconstruction finds extensive applications in the areas of automatic mesh generation and geometric modeling, molecular structure and protein folding analysis. .

The problem of feasibility analysis is analogous to the ideas of surface reconstruction, since the main effort of feasibility analysis lies in identifying and accurately estimating the boundary of the feasible region. In the previous approaches this boundary is approximated by linear inequalities, either by incorporating a hyper-rectangle Swaney and Grossmann (1985) or by describing an approximation of the convex hull Goyal and Ierapetritou (2002) inside the feasible space. These methods can have satisfactory performance in case of convex, connected feasible regions, but will be inaccurate for the cases of nonconvex or disjoint feasible regions. On the other hand, the surface reconstruction scheme can successfully describe both nonconvex and disjoint regions defining the bounding surface by piecewise linear functions.

3.3.1 α shape approach

There are various approaches described in literature for determining the shape of a pattern class from sampled points. Many of these approaches are concerned with efficient construction of convex hulls for a set of points in the plane. Jarvis Jarvis (1977) presented one of the initial works in the area of considering the problem of computing the shape as a generalization of the convex hull of a planar point set. He presented several algorithms based on nearest neighbours that compute the shape of a finite point set. Akl and Toussaint Akl and Toussaint (1978) proposed a way of constructing a convex hull

by identifying and ordering the extreme points of a point set, and the convex hull serves to characterize the shape of such a set. Fairfield Fairfield (1979) had put forward a notion of the shape of a planar set based on the closest point voronoi diagram of the set. Different graph structures that serve similar purposes are the Gabriel graph Matula and Sokal (1980), the relative-neighborhood graph Toussaint (1980) and their parameterized version, the β - skeleton Kirkpatrick and Radke (1985).

A mathematically rigorous definition of a shape was later introduced by Edelsbrunner *et al.* Edelsbrunner et al. (1983). They proposed a natural generalization of the convex hulls which they referred to as $\alpha - hulls$. The α-hull of a point set is based on the notion of generalised discs in the plane. The family of α-hulls includes the smallest enclosing circle, the set itself, and an essentially continuous set of enclosing regions in between these two extremes.

Edelsbrunner *et al.* also define a combinatorial variant of the α-hull called the α-shape of a planar set, which can be viewed as the boundary of the α-hull with curved edges replaced by straight edges. Conceptually, α-shapes are a generalization of the convex hull of a point set $\mathscr{S}$, with α varying from 0 to ∞. The α-shape of $\mathscr{S}$ is a polytope that is neither necessarily convex nor connected. For $\alpha = \infty$, the α-shape is identical to the convex hull of $\mathscr{S}$. However, as α decreases, the α-shape shrinks by gradually developing cavities. When α becomes small enough, the polytope disappears and reduces to the data set itself.

To provide an intuitive notion of the concept, Edelsbrunner describes the space R^3 to be filled with styrofoam and the point set $\mathscr{S}$ to be made of more solid material, such as rock. Now if a spherical eraser with radius α curves out the styrofoam at all positions where it does not enclose any of the sprinkled rocks (the point set $\mathscr{S}$), the resulting object formed will be called an α-hull. The surface of the object can be straightened by substituting straight edges for the circular ones and triangles for spherical caps. The obtained object is the α shape of $\mathscr{S}$. It is a polytope in a fairly general sense : it can be concave and even disconnected; it can contain two-dimensional patches of triangles and one-dimensional strings of edges, and its components can be as small as single points. The parameter α controls the degree of details captured by the α shape.

It is possible to generalize all the concepts involved in the construction of α shape (i.e. α hulls, α complexes, Delaunay triangulation, Voronoi diagrams) to finite set of

points $\mathscr{S}$ in $\mathscr{R}^d$, for arbitrary dimension d. This generalization, combined with an extension to weighted points is developed in Edelsbrunner Edelsbrunner (1992). However, the implementation details of the problem becomes progressively more complex with increasing problem dimensionality, and the worst-case complexity of the problem grows exponentially.

3.3.2 Selection of α

The computed α shape of a given set of sample points explicitly depends on the chosen value of α, which controls the level of details of the constructed surface. Mandal *et al.* Mandal and Murthy (1997) presents a systematic methodology for selecting the value of α in R^2. They visualize the problem of obtaining the shape of $\mathscr{S}$ as a set estimation problem where an unknown set $\mathscr{A} \in \mathscr{B}$ is to be estimated on the basis of finite number of points $X_1, X_2, \ldots, X_n \in \mathscr{A}$. As n increases $\mathscr{S}(n)$ will cover many parts of $\mathscr{A}$ and hence the value of α for $\mathscr{S}(n)$ should depend on the sample size (n), thus α is a function of n. Additionally α should also be a function of the inter-point distance of the sampled n points of $\mathscr{S}(n)$. To account for the dependence on inter-point distance, the authors have constructed the Minimum Spanning Tree (MST) of the sampled data points. If l_n represents the sum of edge weights of the MST, where the edge weight is taken to be the Euclidean distance between the points, then the appropriate value of α for the construction of α shape is given by :

$$h_n = \sqrt{\frac{l_n}{n}} \tag{3.17}$$

where n is the total number of sample points. To illustrate the performance of α shape in capturing the shape of an object, a disjoint, non-convex object is chosen, as illustrated in Figure (3.2). The sampled points represent a 2-d object, which is the input to the α shape construction code. The α shape identifies from the input data set, points which lie on the boundary of the object. These points are joined by a line to describe the surface of the object. The above figure also illustrates the dependence of the captured shape on the chosen value of α. The α value estimated by performing the minimum spanning tree operation is 120, at which value the α shape was found to capture the nonconvex as well as the disjoint nature of the object. By further increasing the value of α the performance

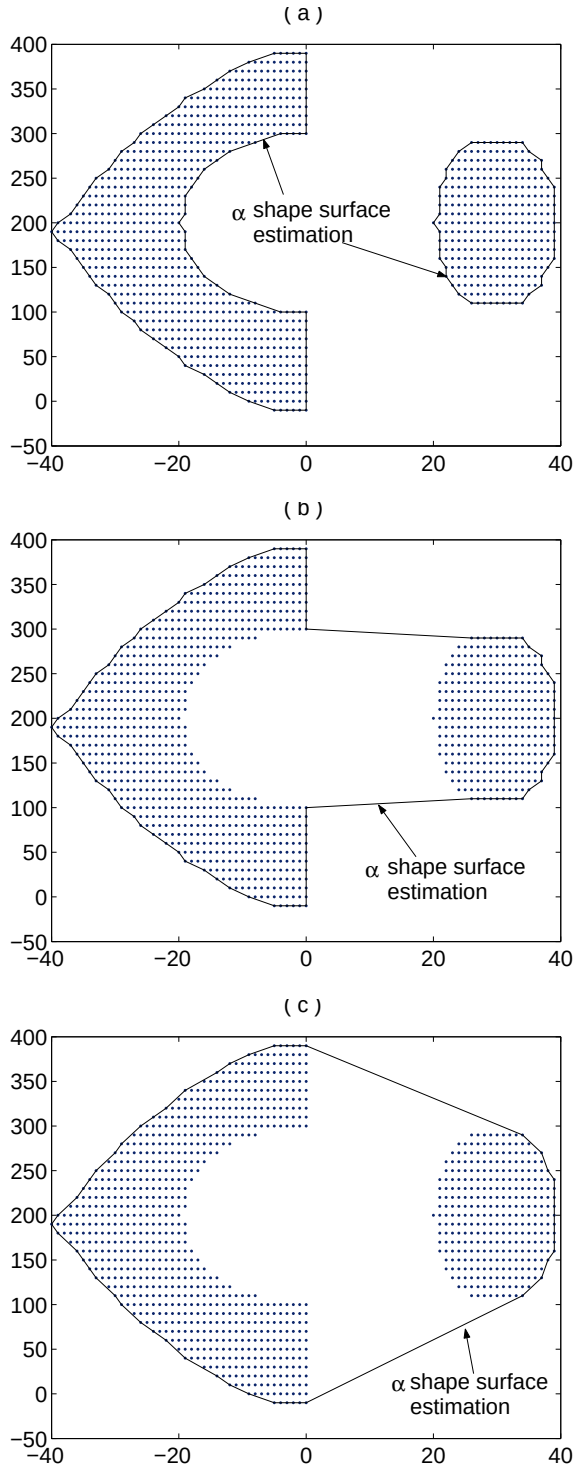

Figure 3.2: Performance of α shape for different α values : (a) 120 (b) 200 (c) 100000

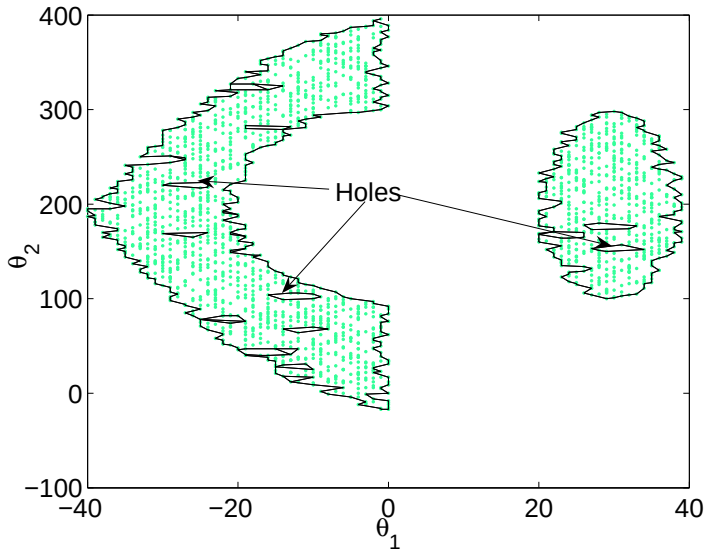

Figure 3.3: Performance of α shape with random points

of α shape deteriorates, as illustrated in Figure (3.2b), and at very high α value the α shape forms a convex hull of the object (Figure (3.2c)). Hence the level of details captured by the α shape strongly depends on the chosen value of α, and progressively decreasing the value of α will capture the shape more accurately. For the case of uniform sampling, where the distance between the sampled points is uniform, the predicted shape is not very sensitive to the value of α for lower α values. However, extreme reduction of the value of α will result in the original data set, and will fail to capture any shape.

In case of random sampling, where the inter-point distance is not constant, the predicted shape is more sensitive to the lower α values. For lower values of α it scoops out holes from within the samples which are not actually present, but is an outcome of sampling. Such an example is illustrated in Figure (3.3) for the same object described by a set of random samples. The shape produced by an α value of 6 has the accurate outside boundary, but it inserted unnecessary holes inside the body. A higher value of $\alpha = 7$ however eliminated the holes. For progressively lower α values, the number of holes go on increasing, and finally for extreme low value it degenerates to original data set without capturing any shape.

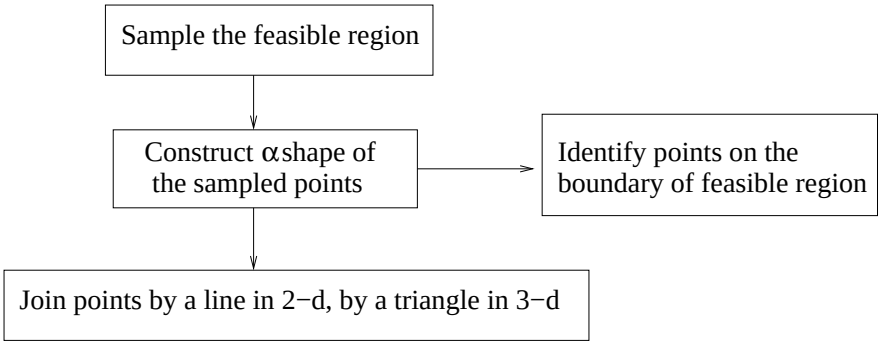

Figure 3.4: Algorithm of feasibility analysis using α shape

3.4 Feasibility analysis using α shape

The overall aim of feasibility analysis is the determination of the range of parameters over which a particular process is feasible. A formal definition of this problem is to obtain a mathematical description of the region in parameter space bounded by the process constraints. This region can be considered analogous to an object, the shape or surface of which can be estimated using the α shape technique. The input to any surface reconstruction algorithm needs to be a set of points representing the object, whose surface needs to be determined. Hence the first step is the generation of good sample data points to represent the feasible region under consideration. The α-shape can then be constructed for the sampled data, using the α estimate obtained from the minimum spanning tree of the data set. The α shape essentially identifies points from the input data set that lie on the surface of the object. These points are then connected by a line in two dimension and triangle in three dimension, giving rise to a polygon enclosing the feasible region. Figure (4.3) illustrates the above mentioned steps.

Having defined the surface or shape of the feasible region, the next step involves the determination of whether a particular point belongs to the feasible region. Since the feasible region has been approximated by a polygon, a simple way to check if a point is inside the polygon is by using one of the point-in-polygon tests Haines (1994). One method to determine whether a point is inside a region is the *Jordan Curve Theorem*, which states that a point is inside a polygon if, for any semi-infinite ray from this point, there is an odd number of intersections of the ray with the polygon's edges (Figure (3.5)).

Conversely, a point is outside a polygon if the ray intersects the polygon's edges an even number of times, or does not intersect at all. Following this, whenever a parameter needs to be checked for feasibility in a polygon estimated feasible region, a semi-infinite ray is drawn from the point in any direction, and the number of intersections is determined, which decides on whether the point is feasible or not.

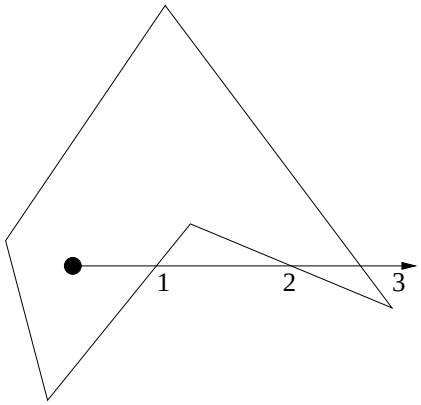

Figure 3.5: Point-in-polygon test: odd number of intersections means point is inside, even number of intersections means point is outside

3.4.1 Sampling technique

Obtaining a good representation of the feasible region is the first and very important step in the α-shape technique of feasibility analysis. In many problems, typically, the feasible region covers only a very restricted region of the entire parameter space. Hence sampling techniques covering the entire range of uncertain parameter proves to be inefficient, particularly when the evaluation of the process constraints is an expensive operation. Most of the common sampling techniques sample the parameter space based on the distribution of the uncertain parameter, which are considered to be uniform for the cases considered here for simplicity of presentation. Under this condition it will lead to uniform sampling of the entire parameter space, irrespective of whether the sampled points are feasible or not. A new sampling technique is thus introduced here, which takes advantage of the fact that typically a small section of the entire parameter space is feasible. The sampling problem is formulated as an optimization problem and is solved using Genetic Algorithm (GA). The use of GA as a solution procedure proves to be very efficient for this problem

since the search scheme has the inherent property of concentrating around regions having good solutions, which is the feasible solution for the problem addressed here.

The purpose of the sampling step is to have a good approximation of the feasible space by minimum evaluation of the expensive feasibility function. The formulation of the sampling problem as an optimization problem is given by:

$$\begin{aligned} &\max_{\theta} V_{feas} \\ subject\,to\, &(f_1)_\theta \leq 0 \\ &(f_2)_\theta \leq 0 \\ &\vdots \\ &(f_n)_\theta \leq 0 \end{aligned} \tag{3.18}$$

where V_{feas} is the volume of the feasible region, evaluated by constructing the α-shape using the sampled feasible points. The optimization variables are the parameter values θ, which are sampled by GA to optimize the objective, and $f_1, f_2 \ldots, f_n$ are the constraints of the feasibility problem evaluated at θ. However, in this formulation there is no optimal value of the variable θ which will maximize the volume, but we are interested in the entire sampled set of feasible θ values, using which the volume is evaluated by constructing an α-shape over the entire set of feasible θ values. Since the objective is to maximize the volume of the feasible space, whenever a chosen value of θ satisfies the constraint functions, the volume is evaluated to update the objective function. When the value is not feasible there is no need to reevaluate the volume since it will not change, but the fitness function is penalized by assigning it a small value. By solving this problem using GA reduces the required number of function evaluations by minimizing the unnecessary evaluation of infeasible parameter space. In order to solve the optimization problem by GA, the optimization variables are encoded as a string of bits, and these strings are appended together to form a chromosome. The solution procedure starts by generating a population of solutions, where each individual in the population has a particular chromosome value which can be decoded to evaluate the parameter values and the objective function, also called the fitness function. As shown by DeJong DeJong (1975), large population sizes exhibit slower convergence than small population, but they tend to converge to better

solution. In the interest of balancing execution time and optimality, the population size is chosen to be of the order of the chromosome size, as suggested by Edwards *et al.* Edwards et al. (1998).

$$n_{chromosome} < n_{population} < 2n_{chromosome} \tag{3.19}$$

The populations are evolved through several generations, following rules like reproduction, crossover, mutation, until the objective function cannot be improved any further. The primary objective of reproduction operator is to emphasize good solutions and eliminate bad solutions in a population. This is achieved by first identifying above-average solutions in a population, making multiple copies of the good solutions and eliminating bad solutions from the population in order to accommodate multiple copies of the good solution. Some common methods for achieving this is by *tournament selection*, *proportionate selection*, *ranking selection* etc. Goldberg (1989). In all the examples presented in this work, tournament selection was chosen to be the reproduction operator. While reproduction can make more copies of the good solution and eliminate bad solution, however, it cannot create a new solution. The crossover operator is applied next to take care of that, where two strings are picked randomly from the mating pool and some portions of the strings are swapped among themselves to create two new strings. If the new strings created by a crossover are good, there will be more copies of them generated by the reproduction operator in the next mating pool. Otherwise if the new strings are not good, they will not survive beyond next generation, since reproduction will eliminate them. A uniform crossover between randomly selected pairs is used for this work.

The parameters chosen for GA operations largely govern the computational time as well as the quality of the solution. If the selection operator emphasizes too much on the population-best solution by assigning many copies of it, then the population loses its diversity very quickly. The crossover and mutation operators should be strong enough to retain the diversity of solution and create solutions fairly different from the parent solution. In the absence of this, the simulation can converge to suboptimal solution. On the other hand, if the reproduction operator is weak and the crossover operator very strong, the GA's search procedure behaves like a random search process. The GA parameters chosen for all the examples presented here are $p_{crossover} = 0.5$ and a small mutation probability $p_{mutation} = 0.02$.

The working principle of GA is that by applying these three operators, the number of strings with similarities at certain string positions are increased from one population to the next. These similarities, referred to as *schema* in GA literature, represents a set of strings with similarity at certain string positions. Thus the *schema* can be thought of as representing certain regions in the search space, or specific ranges of the parameter value. Hence by having more copies of a schema with a better function value, one can reach the optimal solution without searching the entire variable space, but by manipulating only a few instances of the search space.

This feature of GA is of particular importance for the present problem since only a limited region of the variable space is feasible, and exploring the entire variable space to have an idea of the feasible region becomes computationally expensive. As mentioned above, the working principle of GA is based on generating multiple numbers of the good solutions. Hence by evaluating the volume for each of the feasible parameter value (θ) will reduce the efficiency of the procedure because of the repetition of the same solutions. To avoid this, a memory of the sampled parameter value is maintained and updated. For every generated chromosome in the population of the GA simulation, the stored parameter values are searched to check for uniqueness of the new solution. If the new solution is unique, then the constraints are evaluated, else it is updated from the memory.

3.4.2 Range of validity of reduced kinetic model

Figure (3.6) represents a typical feasible region of reduced CH_4 mechanism consisting of 17 species and 59 reactions, where the detailed model consists of 53 species and 325 reactions. The nominal point of reduction for this problem is $O_2 = 0.005$ mass frac., $CH_4 = 0.38$ mass frac., T = 950K. As illustrated in Figure (3.6), the feasible region can be highly nonconvex, even disjoint, for which cases the conventional techniques cannot be used. The problem is solved using the convex hull approach, where the boundary points are identified by moving in different directions from the nominal point. Figure (3.7) illustrates the predicted feasible region by the convex hull. The reduced mechanism is feasible in two disjoint regions, a small region in the low O_2 concentration, and considerable portion towards the higher O_2 concentration. However, the nominal point lies on the low O_2 region, hence restricting the convex hull estimate within this small portion, and preventing

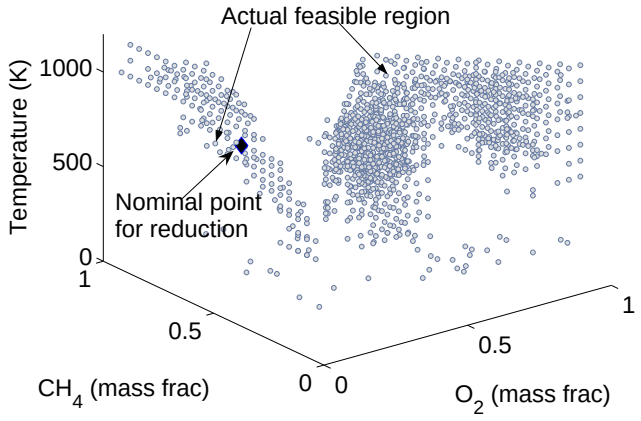

Figure 3.6: Feasible region of a reduced model of GRI-3.0 mechanism involving 17 species and 59 reactions

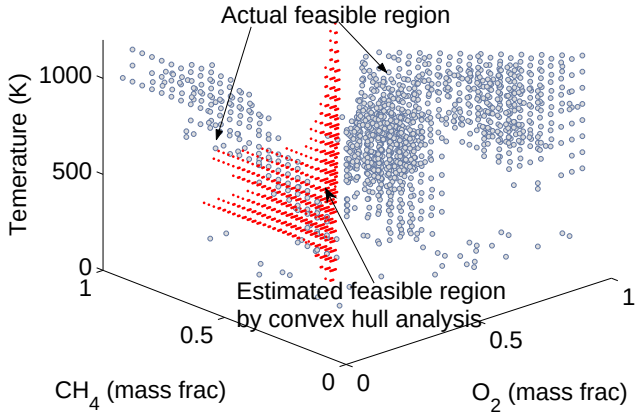

Figure 3.7: Predicted feasible region of the reduced model obtained by convex hull approach

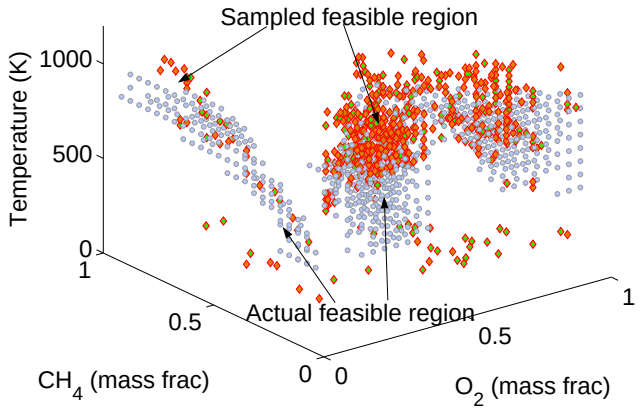

Figure 3.8: Sampled feasible region of a reduced model of GRI-3.0 mechanism

it from providing any estimate of the major range of feasible operation. Figure (3.6) is generated by performing grid search over the variable space, where at each point one needs to determine the deviation of the reduced model from the detailed mechanism due to change in conditions of species concentration and temperature. This evaluation is an expensive operation, and performing grid search over the entire variable space is not feasible. The sampling technique described in section (3.1) is used to have a representation of the feasible space. The three variables, O_2 mass fraction, CH_4 mass fraction, and temperature are coded using 5 bits for each parameter, giving rise to 15 bit chromosome. The GA simulation is run with a population size of 20, evolved through 250 generations, which will require 5000 function evaluations. However, due to the retained memory of the previous calls, the number of function evaluations were reduced to 1809, of which 778 points were determined to be feasible. The generation of this feasible region using GA requires approximately 25 hrs, whereas using random sampling to generate 778 feasible points requires 70 hrs. Figure (3.8) illustrates the sampled feasible region as compared to actual feasible region obtained by grid search. An α shape is then constructed with these sampled data set. In a three dimensional space α shape identifies points on the boundary of the object, which are to be joined in a triangle to form the surface of the object. Having obtained the surface of the feasible region, the next step is determination of whether a point lies inside the feasible region, which can be done using the point-in-polygon test. Using this procedure the predicted feasible region is constructed, as illustrated in Figure

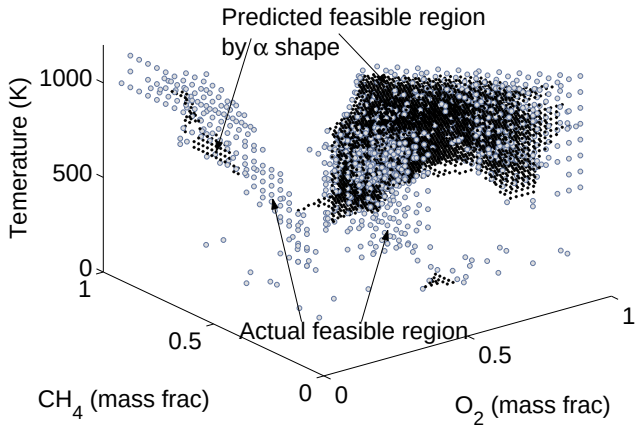

Figure 3.9: Predicted feasible region of a reduced model

(3.9). The α shape procedure is found to capture 71% of the actual feasible space, which can still be improved by generating more sample points by allowing the GA simulation of the sampling step to evolve for more generations. This is a large improvement over the convex hull approach, which covers only 3% of the overall feasible space, mainly because of the disjoint nature of the feasible space. Moreover, as illustrated in Figure (3.7), the convex hull approach also overestimates the feasible region, which is a consequence of the nonconvexity of the feasible space. Since α shape can accurately capture the nonconvexity of the shape, it results in no overprediction.

3.5 Summary

An alternative formulation is presented for feasibility analysis of reduced mechanisms using the surface reconstruction ideas. The problem definition is to evaluate and quantify the uncertain parameter range over which the reduced model retains its validity. In the present approach the feasible region is viewed as an object, with the constraints defining the boundary of the object. The surface reconstruction ideas are used to define the shape of the object. The procedure starts by first sampling the feasible region to obtain a representation of the feasible space. An α shape is then constructed of the sampled points, which identifies points forming the boundary of the object. These points are joined to have a polygonal representation of the feasible region. Finally, determination of whether a

point is feasible or not can be done by a point-in-polygon check. The presented procedure was found to have much better performance over conventional techniques of feasibility analysis.

The multiperiod formulation enables generating reduced mechanisms possessing accuracy over desired range of species concentration and temperature. Such a multiperiod formulation was also found to overcome the problem of presence of uncertainty in the determination of kinetic parameters, since it enables determination of reduced reaction set valid over a given range of rate constants. Simulations performed for CO/H_2 and H_2/O_2 system were found to have good agreement with the SRSM results.

Chapter 4

Formulation of Adaptive Reduction

Having determined an efficient scheme for obtaining reduced kinetic models and evaluating the range of validity, the next step is the integration with reacting flow simulation. The reactive flow models typically span a broad range of conditions with respect to species concentration and temperature. The detailed model retains information regarding kinetic behavior of the system under all the different conditions of species concentration and temperature. However, when the detailed model is reduced, the reduced model loses such generality, since it retains information of system behavior under specific conditions given by its range of validity. If the same reduced model is used under all the conditions encountered in the reactive flow model irrespective of its validity, it will incorporate inaccuracy in the predictive capacity of the simulation. To overcome this problem the adaptive reduction scheme is proposed in this work, where the aim is to adapt the reaction model to the changing condition of the flow simulation. This is achieved by generating multiple reduced models addressing different conditions of the system. The flow simulation will use a particular reduced model only where it is feasible, meaning it retains its accuracy in prediction of the actual system behavior. Whenever the flow simulation encounters a condition for which the present selection fails, it will search for a different reduced model valid for such condition, and integrate it.

Thus, the main aim is to generate a library of reduced model, the feasible region of which together cover the entire range of conditions encountered in the reactive flow simulation. However, this requires *apriori* knowledge of the accessed region of the detailed reactive flow simulation involving detailed kinetic model, which is not possible. An alter-

native method is to have an estimate of the accessed region, which can be obtained by solving the detailed flow simulation with a reduced mechanism or a simplified flow simulation with detailed kinetic mechanism. In the present work the stochastic simulation of zero-dimensional reactor model is used for the estimation of the accessed region, primarily because it is computationally tractable even with the detailed kinetic model, and covers a broad range of conditions in the composition state space.

4.1 Stochastic reactor simulation

The stochastic reactor simulation falls in the broad category of probability density function (PDF) approach to model turbulent flows. At each point in the flow field, a complete statistical description of the state of the fluid is provided by the velocity-composition joint pdf. This is the joint probability density function (pdf) of the three components of the velocity and of the composition variables (species mass fraction and enthalpy). The principle method is to solve a modelled transport equation for the velocity-composition joint pdf, where the effects of convection, reaction, body forces and the mean pressure gradient are explicitly considered and do not need to be modeled (Pope (1985)).

In the present work two different alternatives are evaluated for the estimation of the accessed region, that of the homogenous flow simulation of a partial stirred reactor with micromixing described by the Interaction-by-Exchange-with-Mean (IEM) model and the pairwise mixed stirred reactor model.

4.1.1 Stochastic simulation of PaSR

The salient feature of the PaSR model is the unmixed nature of the reactive fluids at the molecular level. Inside the reactor, the mean thermo-chemical properties are assumed to be spatially homogeneous but imperfectly mixed at molecular level. That is, the reactive fluids are not completely diffused into each other at the molecular level, but their mean values are uniform throughout the reactor due to turbulent stirring. With the above assumption, Curl (1963) derived the probability density function (pdf) evolution equation for a single reactive scalar. From general view of modeling turbulent reactive flow, PaSR can be considered as a single grid cell embedded in a large computational

scheme. Therefore, PaSR offers a good test bed for exploring the influence of the unmixed nature on chemical kinetics, for evaluating the performances of reduced chemistry, and for assessing various mixing models. A stochastic modeling approach for PaSR has been developed by Correa (1993) for premixed combustion and by Chen (1997) for nonpremixed combustion, where the pdf is represented by an ensemble of N_p particles, each having a unique composition. The pdf $P(Y_k)$ of mass fraction Y_k of the species in the reactor is represented by the N_p ensemble :

$$Y_k^{(1)}, Y_k^{(2)}, ..., Y_k^{(N_p)}, k = 1, ..., N_s \tag{4.1}$$

A time marching scheme is used for the stochastic simulation which is carried out by the following sequential procedure:

1. Throughflow is simulated by randomly selecting fluid particles from the ensemble of N_p particles at the specified mass flow rate. The properties of these selected particles are set to the properties of the incoming mixture, and their age is reset to zero. The number of fluid particles to be replaced at each time step (Δt) is given by (Borghi, 1988):
$$N_{replaced} = \frac{\Delta t}{\tau_{res}} N_p \tag{4.2}$$

2. Fluid particles in the reactor are allowed to mix at the prescribed mixing frequency. This can be achieved by using either Coalescence-Dispersion (CD) or IEM as the micromixing model.

3. The mixed fluid particles are then allowed to react according to chemical kinetic rate equations.

Modelling PaSR with IEM model

While using IEM to model molecular mixing, reaction and mixing are considered simultaneously, and fractional time stepping is not required. The governing equation for each particle is given by:

$$\frac{dY_k^{(n)}}{dt} = -\omega(Y_k^{(n)} - \overline{Y_k}) + R_k^{(n)} M_k / \rho^{(n)}, k = 1, ..., N_s; n = 1, ..., N_p \tag{4.3}$$

where ω is the mixing frequency, $R_k^{(n)}$ is the molar production rate of specie k per unit volume of the n^{th} particle, M_k is the molecular weight of specie k and $\rho^{(n)}$ is the density

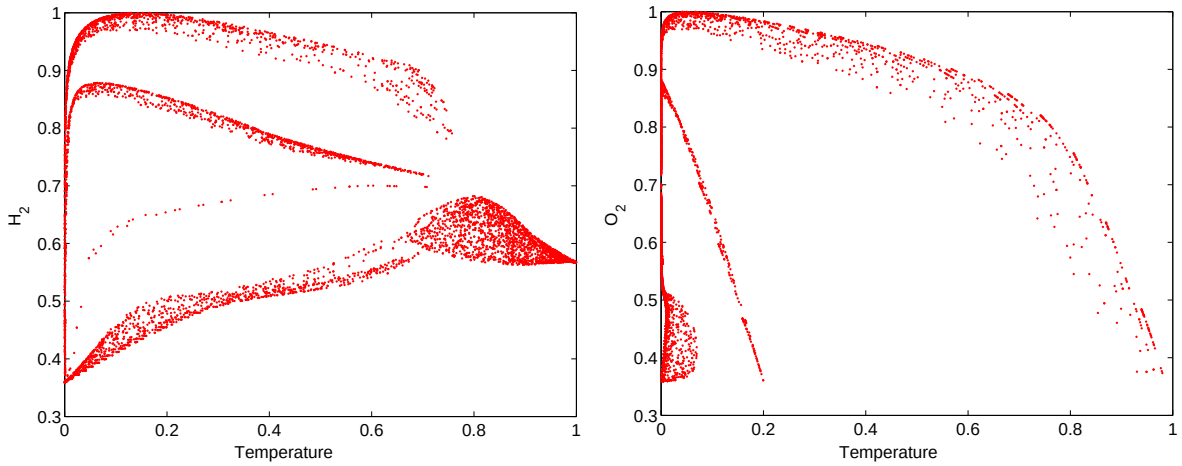

Figure 4.1: Accessed region for a PaSR (a) projection in Temperature - H_2 plane (b) projection in Temperature - O_2 plane

of the n^{th} particle. The corresponding equation for the particle temperature is:

$$C_p \frac{dT^{(n)}}{dt} = -\omega \sum_{k=1}^{Ns} Y_k^n (h_k^{(n)} - \overline{h}_k) + \sum_{k=1}^{Ns} h_k^{(n)} R_k^{(n)} M_k / \rho^n \tag{4.4}$$

The first term on the right hand side of Equation (4.3) describes linear deterministic relaxation to the mean, which is the main characteristic of the IEM model. The second term is the reaction rate term for specie k, which introduces significant complexity and stiffness.

For each of the N_p particles, Equation (4.3) is solved for each of N_s species and Equation (4.4) for temperature. The quantities required in the IEM model are updated from the ensemble. This procedure is repeated until a stochastic steady state is achieved. If, however, a large change occurs in the current particle (the one under integration), the mean quantities will be affected during the current time step and the IEM model term will be incorrect. This places a restriction on the maximum allowable change within the global time step, and hence a restriction on the maximum allowable time step. PaSR simulation is performed with progressively smaller time steps until convergence of mean statistics is established.

4.1.2 Stochastic simulation of PMSR

At any time t, the PMSR consists of an even number N of particles, the i^{th} particle having composition $\phi^{(i)}(t)$. The overall simulation of PMSR proceeds in the same way as for PaSR, where all the reactor particles are assigned initial conditions at $t = 0$, and then the simulation is advanced in discrete time steps until a statistically stationary state is attained. Between these discrete times, the composition evolves by a mixing fractional time step and a reaction fractional time step.

In PMSR, the reactor particles are arranged in pairs such that particles 1 and 2, 3 and 4, ..., $N-1$ and N are partners. The mixing fractional step consists of pairs (p and q, say) evolving by a simple first order linear model :

$$\begin{aligned} \frac{d\phi^{(p)}}{dt} &= -(\phi^{(p)} - \phi^{(q)})/\tau_{mix} \\ \frac{d\phi^{(q)}}{dt} &= -(\phi^{(q)} - \phi^{(p)})/\tau_{mix} \end{aligned} \tag{4.5}$$

where τ_{mix} is the specified mixing timescale. The other physical processes present in the PMSR model are inflow and outflow to and from the reactor and reassignment of particle pairs, which ensures mixing between all particles in the reactor. With τ_{res} being the specified residence time, outflow and inflow consists of selecting $1/2N\Delta t/\tau_{res}$ pairs at random and replacing their compositions with inflow compositions, which are drawn from a specific distribution. With τ_{pair} being the specified pairing timescale, $1/2N\Delta t/\tau_{pair}$ pairs of particles (other than the inflowing particles) are randomly selected for pairing. Then these particles and the inflowing particles are randomly shuffled so that they have the probability of changing partners. Figure(4.2) illustrates the accessed region for PMSR in temperature-H_2 and temperature-O_2 space. It is observed that a considerable portion of the temperature and species composition space is accessed by the PMSR simulation, and hence provides satisfactory initial estimate of the composition space accessed in a more rigorous reactive flow model.

4.2 Clustering the accessed space

Having obtained an estimate of the accessed composition space, the next objective is to generate reduced reaction models which can cover the entire accessed space. To ac-

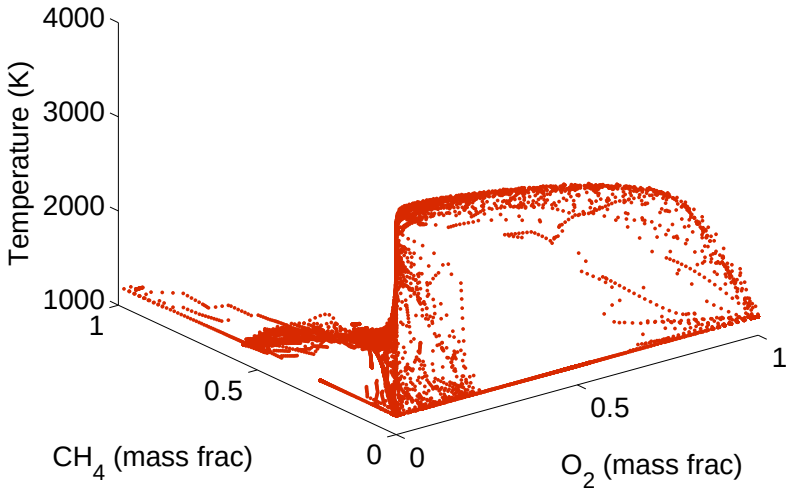

Figure 4.2: Accessed region for a PMSR in Temperature - CH_4 - O_2 space

complish this, one needs to identify nominal points at which such mechanism reduction needs to be performed. This can be obtained by clustering the data of temperature and species concentration to identify patterns in the data set and representative points for such patterns.

Data Clustering is a branch of data mining problem. Given a large set of multi-dimensional data points, the data space is usually not uniformly occupied. *Data Clustering* identifies the sparse and the crowded places, and hence discovers interesting data distributions and patterns in the underlying data. The problem of clustering can be defined as follows: given n data points in a d- dimensional metric space, partition the data points into k clusters such that the data points within a cluster are more similar to each other than data points in different clusters. Clustering techniques have been studied extensively in many different fields such as statistics, machine learning, data mining, with numerous methods proposed and studied. Existing clustering algorithms can be broadly classified into *partitional* and *hierarchical*. Partitional clustering algorithms attempt to determine k partitions that optimize a certain predefined criterion function. A hierarchical clustering is a sequence of partitions in which each partition is nested into the next partition in the sequence. An *agglomerative* algorithm for hierarchical clustering starts with the disjoint set of clusters, which places each input data point in an individual clus-

ter. Pairs of items or clusters are then successively merged until the number of clusters reduces to k. At each step, the pair of clusters merged are the ones between which the distance is the minimum. The widely used measures for distance between clusters are as follows :

$$d_{mean}(C_i, C_j) = ||m_i - m_j||$$
$$d_{ave}(C_i, C_j) = 1/(n_i n_j \sum_{p \in C_i} \sum_{p\prime \in C_j} ||p - p\prime||$$
$$d_{max}(C_i, C_j) = \max_{p \in C_i, p\prime \in C_j} ||p - p\prime||$$
$$d_{min}(C_i, C_j) = \min_{p \in C_i, p\prime \in C_j} ||p - p\prime||$$

where, m_i is the mean for cluster C_i and n_i is the number of points in C_i. Hence, with d_{mean} as the distance measure, at each step, the pair of clusters whose centroids or means are the closest are merged. On the other hand, with d_{min} as the distance measure, the pair of clusters merged are the ones containing the closest pair of points. The performance of a particular clustering algorithm or the distance measure to be employed depends heavily on the nature of the dataset used. All of the above measures usually yield similar results when the clusters are compact and well separated. However, if the clusters are close to one another, or if their shapes and sizes are not hyperspherical and uniform, the results of clustering can vary quite dramatically. However, neither the centroid based approach (using d_{mean}) nor the all-points approach (using d_{min}) works well for non-spherical or arbitrary shaped clusters. The shortcoming of the centroid-based approach is that it considers only one point as representative of a cluster, which is the cluster centroid. For a large or arbitrary shaped cluster, the centroids of its subclusters can be reasonably far apart, thus causing the cluster to be split. The all-points approach, on the other hand, considers all the points within a cluster as representative of the cluster. This approach makes the clustering algorithm extremely sensitive to outliers and to slight changes in the position of the data points. In recent years, a number of clustering algorithms have been proposed for large databases. Raymond and Han (1994) proposed a partitional clustering method for large datasets, where each cluster is represented by its *medoid*, the most centrally located point in the cluster, and the objective is to find the k best medoids that optimize the criterion function. In Ester et al. (1993) proposed the CLARANS algorithm which outperforms the traditional *k-medoid* algorithm, but its runtime cost

could be prohibitive for large datasets. In Zhang et al. (1996) the authors presented a clustering method called BIRCH, which first preclusters the data into sub-clusters, then treats each of the sub-clusters as representative points to run the hierarchical clustering algorithm. BIRCH and CLARANS work well for convex or sperical clusters of uniform size, but are not suitable for nonspherical clusters having varied sizes.

As observed in Figures (4.1) and (4.2), the data set in the present problem, which is the accessed region determined by the PMSR in the temperature-composition space, is large and of arbitrary shape, hence eliminating the possibility of using the above algorithms. For clustering such arbitrary shaped collection of points, a density-based algorithm called DBSCAN was proposed in Ester et al. (1996), which works on two user defined parameters: the radius *Eps* of the neighborhood of a point and the minimum number of points *MinPts* in the neighborhood. While DBSCAN can find clusters with arbitrary shapes, it has the problem of being extremely sensitive to the parameters and not being very robust. A recently proposed hierarchical based algorithm named CURE (Clustering Using Representatives) Guha et al. (1998) has the salient features of recognizing arbitrarily shaped clusters, having linear storage requirement and time complexity of $O(n^2)$ for low-dimensional data, and is also stable. CURE adopts a middle ground between the centroid-based and all-point extremes. It starts by selecting a constant number c of well scattered points, which are next shrunk towards the centroid of the cluster by a fraction α. These points are used as representative of the cluster, and the clusters with the closest pair of representative points are merged at each step of the algorithm. The c representative points help in capturing the physical shape and the geometry of the cluster, and shrinking these points gets rid of surface abnormalities and mitigates the effect of outliers. The kind of clusters identified by CURE can be tuned by varying the value of α between 0 and 1. It reduces to centroid-based algorithm for $\alpha = 1$, and to all points approach for $\alpha = 0$. It uses space that is linear in input size n and has a worst case time complexity of $O(n^2 log n)$. In the present work CURE has been used to cluster the datasets, and it was observed that considering larger number of representative points indeed captured the shape of the cluster better than having a single point. However increasing the number of representative points to more than 5 deteriorated the results.

4.3 Generation of library of reduced model

Having obtained the clusters, and the representative points for each cluster, one of the cluster centers is chosen at which mechanism reduction is performed following the procedure illustrated in Chapter 2, where first the detailed kinetic model is formulated for species reduction at the initial condition given by the cluster center, to arrive at an intermediate reduced model. This model is further reduced by the formulation of reaction reduction, to come up with the final reduced kinetic model at the particular initial condition. The next step is the determination of the range of validity of the reduced model within which it retains the desired accuracy. This requires an estimate of the feasible region, which can be obtained by sampling the temperature-composition space following the technique described in Section 3. In order to obtain a mathematical definition of this feasible space, an α shape is constructed, which identifies the boundaries of the feasible space. The accessed data points are then checked to identify points which lie inside the generated feasible region using the point-in-polygon strategy. The feasible points are removed and the updated data set is reclustered to obtain another nominal point for reduction. This procedure is followed iteratively, as illustrated in Figure (4.3) until enough reduced mechanisms are generated to cover the entire accessed region. The reclustering procedure is necessary since the feasible points for a particular reduced mechanism can cover an entirely different region than defined by the initial cluster for which the nominal point was the cluster center. Hence by the proposed iterative procedure the optimum number of reduced mechanisms covering the entire accessed space of the PMSR is obtained.

For the present simulation for methane combustion, a total of 18 reduced sets were generated covering 76 % of the region accessed by the PMSR model. All the reduced models were obtained by running GA with a population size of 10, evolved through 500 generations, with an allowable error of 0.01. Figure (4.4) illustrates the different ranges of conditions addressed by different reduced model.

The details of the size of all the reduced models is given in Table (4.1). It also compares the average CPU time required to integrate each of the reduced model. The CPU time required to integrate the detailed GRI-3.0 mechanism is 7.99 seconds, which is much higher than the reduced models.

All of these reduced models are obtained under different conditions of temperature and

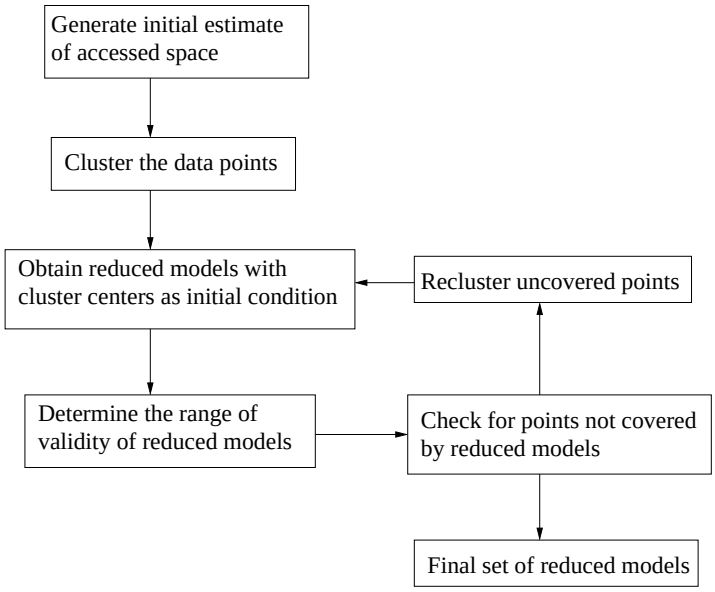

Figure 4.3: Overall algorithm for adaptive reduction

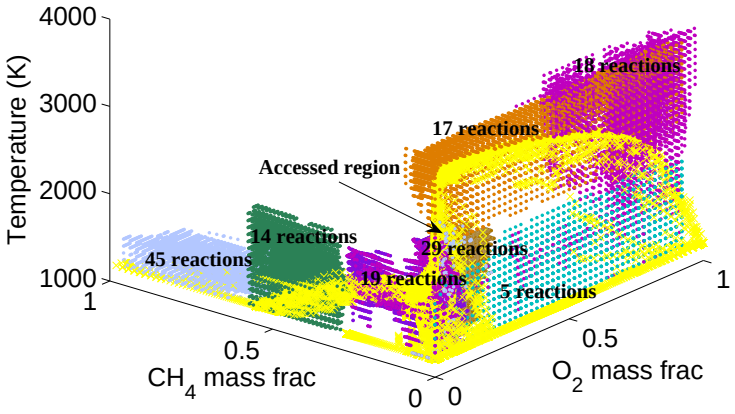

Figure 4.4: Range of conditions addressed by different reduced model

Reduced mechanism	*Size of mechanism*		*Single integration*
	$N_{species}$	$N_{reactions}$	CPU (s)
1	24	45	0.265
2	25	65	0.605
3	14	14	0.004
4	18	19	0.0064
5	29	105	0.0484
6	21	29	0.1884
7	27	64	0.0258
8	28	68	0.0292
9	27	82	0.6964
10	17	23	0.6048
11	24	47	0.02246
12	25	58	1.2008
13	26	48	1.1306
14	27	82	2.1998
15	6	5	0.0146
16	9	17	0.0368
17	13	18	0.0596
18	19	24	0.0504

Table 4.1: Reduced models used for adaptive simulation

fuel and O_2 concentration. In order to ensure that the models indeed capture the physics of the system the reduced models were tested for the known behavior of the system. For example, the nitrogen oxide formation is known to be absent at low temperatures and takes place only at higher temperature. Similar behavior is observed in the reduced models, where the nitrogen oxide reactions were absent from the low temperature reduced models and appear in the high temperature mechanisms. Also, the high temperature mechanisms included the endothermic dissociation reactions, which is absent from the low temperature mechanisms, which is also a physical behavior. The reduced models obtained at high temperature is also consistent with the high-temperature methane oxidation mechanism discussed in Glassman Glassman (1996).

Once sufficient number of reduced reaction models have been developed to cover the entire estimated accessed region, the next step is the incorporation of the reduced sets in the reactive flow models. Before incorporating the library of reduced model in the detailed flow simulation, it is first incorporated in the developed PMSR model, since it offers a perfect testbed for judging the performance of the proposed scheme.

As mentioned before, the PMSR simulation is a time marching scheme, where the incremental time step is split into the mixing time step and the reaction time step. For such a fractional time stepping approach, the flow time stepping will remain unaltered. This time step will result in a set of species concentrations and temperature which are passed on to the reaction time step, at which the system will react under the conditions obtained from flow time step. This reaction step requires the integration of a set of coupled stiff ODE's, which needs to be integrated over the reaction time step. While using the detailed model for kinetic source term, all the N_s ODE's consisting of N_R reaction terms need to be integrated. The objective of the reduced model is to reduce the number of ODE's and their coupling by eliminating species and reactions participating in the source term. While using a single reduced reaction model over the entire flow simulation, the same set of reduced ODE's needs to be integrated at the reaction step. In the adaptive chemistry scheme, however, there is a library of mechanisms from which the most appropriate one needs to be selected and integrated. Hence at every time it is likely that a different set of reduced ODE's are integrated. The accuracy of the reduced model depends solely on the initial condition of the species concentration and temperature at which it is used. Also each reduced set is characterized by an α shape defining the

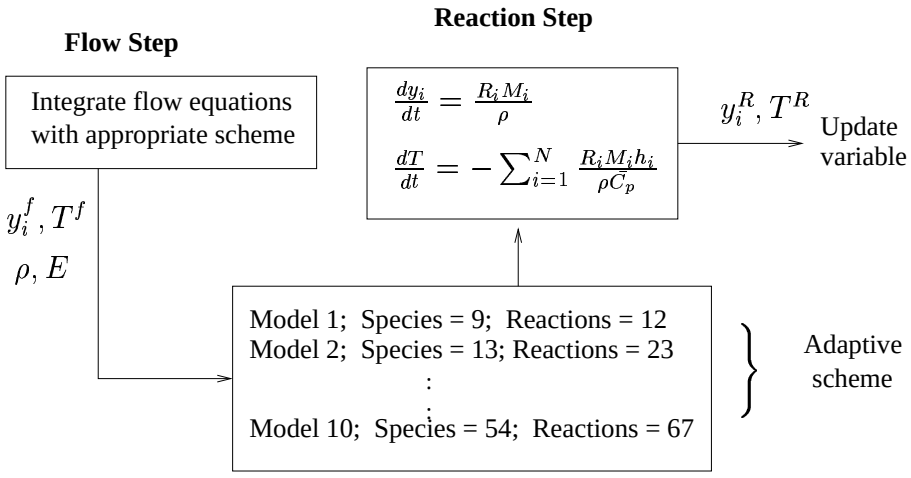

Figure 4.5: Integration with flow simulation

range of conditions over which it is accurate. Hence to select an appropriate reduced mechanism during the PMSR simulation, one needs to check the feasible region of all the mechanisms by performing the point-in-polygon test, to determine one which is feasible at the local condition (Figure (4.5)). Hence, the flow time step will involve the solution of all the species of the detailed mechanism, while the reaction time step will consider only those species present in the selected reduced model, and the concentration of all the other species will remain unaltered. This procedure was followed for PMSR simulation for methane combustion. The library of reduced sets presented in table (4.1) is used along with their corresponding feasible region, which is the information of points forming the boundary of their range of validity. Depending on the local condition of the reactor, different reduced models were chosen by the flow simulation.

As is observed in the figure, most of the reduced models have overlaps in the feasible region. This means that more than one reduced model is valid under certain conditions. When such a situation arises, it is judicious to choose the smallest of all the valid models. With this aim, the library of the models are arranged according to increasing number of reactions. When the flow simulation accesses this library, it will come out of the library on identifying first valid model. This procedure was followed for the PMSR simulation of CH_4 combustion, when the 18 reduced models were found to cover 76% of the conditions encountered by the flow simulation. For the remaining 24% of the conditions there were no valid reduced model in the library, hence the simulation integrated the detailed model

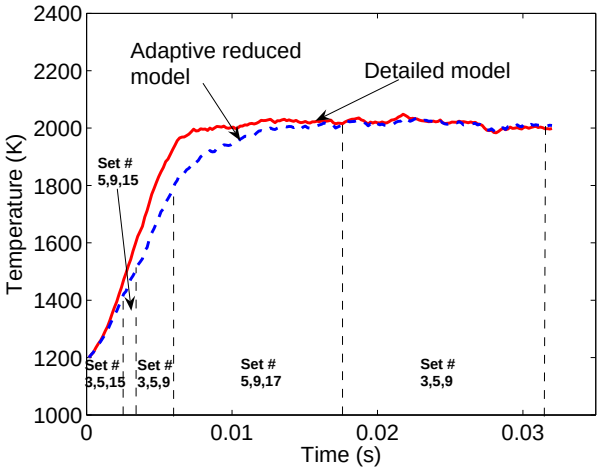

Figure 4.6: Important reduced models selected at different time intervals

for these conditions.

For the PMSR simulation, at every time step all the reactor particles are under different conditions of species concentration and temperature, depending on which it selects an appropriate mechanism. Hence at every time step each of the reduced models were selected, but with different frequency. The reduced models chosen with higher frequencies can be considered to affect the reactor condition the most. Figure (4.6) illustrates the evolution of the three most important reduced models at different time intervals. Similar simulation was also performed using a single reduced set for the entire flow simulation and Figures (4.7) and (4.8) illustrates the performance of adaptive reduction in the prediction of the species and temperature profiles as compared to using a single reduced model. The adaptive scheme could predict the temperature profile with an error of 0.75 %, whereas the single reduced model had an error of 11 %. The prediction of CH_4 profile was comparable for both the cases, where the adaptive scheme had an error value of 0.1387, and the single reduced model had that of 0.1125. The prediction of both the H and H_2 profiles was more accurate for adaptive scheme, having an error of 9% and 7% respectively, while the corresponding values for single reduced model was 32% and 21%. The average size of the reduced model used for the adaptive scheme is approximately 54, while that of the single model was 59. This shows that by adapting the reduced model to the changing condition of the flow simulation, greater accuracy can be obtained with the same dimension of the reduced model.

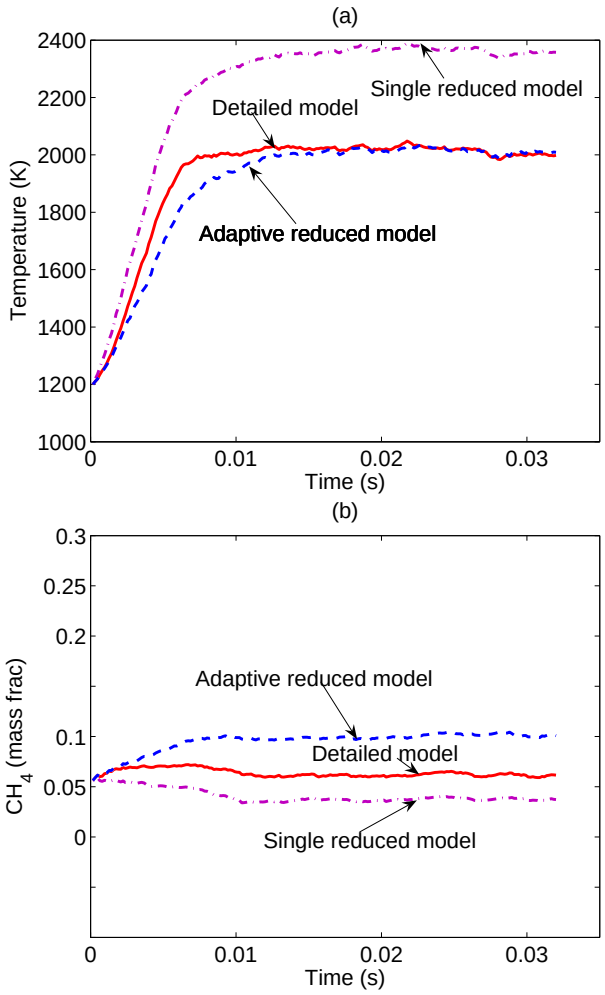

Figure 4.7: Performance of adaptive reduction in the prediction of (a) temperature and (b) methane profile

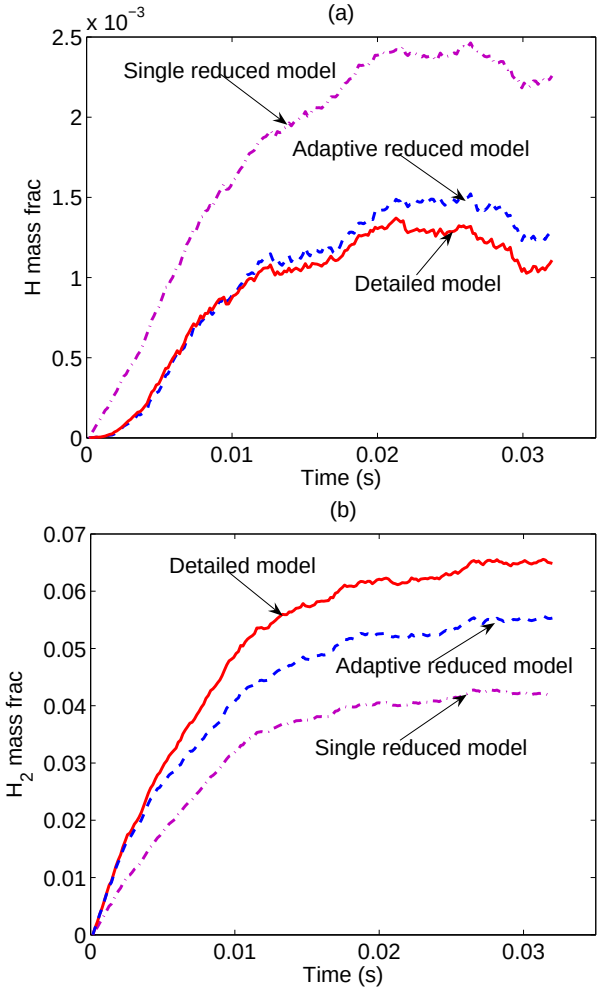

Figure 4.8: Performance of adaptive reduction in the prediction of (a)H and (b) H_2 profile

4.4 Summary

In the proposed work an adaptive reduction scheme is developed to replace the detailed complex kinetic network with a set of simple reduced networks, which can predict the behavior of the detailed model with high accuracy within a limited range of conditions. The procedure involves generating an initial estimate of the range of conditions encountered in a practical reactive flow simulation. This is followed by identification of nominal points at which mechanism reduction needs to be performed. Using the two-step mechanism reduction scheme discussed in Chapter 2, a reduced model is obtained at each of the cluster centers. Each of these reduced models are then analysed following the feasibility analysis technique developed in Chapter 3. This procedure gives rise to a library of reduced models, the feasible region of which together covers the accessed region of the PMSR model. The integration of the adaptive chemistry scheme with the pairwise mixed stirred reactor is also presented. Since the PMSR spans a large area in the composition-temperature space, it provides a stringent test for any reduced chemistry scheme. The excellent performance of the proposed scheme in the PMSR simulation does illustrate the potential of the approach and indicates its suitability for using this approach in a more rigorous flow simulation.

The overall approach of the adaptive scheme is to develop multiple reduced models based on the conditions encountered by the PMSR simulations, and use these models in different reactive flow simulations. However, it is possible that the conditions encountered in the flow simulations where the adaptive scheme is applied is different from that of the PMSR model. In such a case none of the reduced models in the library will be chosen to replace the detailed model. To circumvent this problem, the feasibility analysis is performed for the entire range of CH_4, O_2 and temperature conditions, and is not limited by the conditions accessed by the PMSR. Hence the feasible region of the developed models cover a much larger range of conditions, thereby increasing the probability of choice of a reduced model while solving different reactive flow models.

Chapter 5

Integration with Flow Simulation

Having determined an efficient scheme for obtaining reduced kinetic models and evaluating the range of validity, the next step is the integration with the reacting flow simulation. This requires generation of a library of reduced kinetic models, the feasible region of which can cover the entire range of conditions to be encountered in the reactive flow simulation. An efficient algorithm is presented for identification of nominal points for performing reduction and subsequent feasibility analysis. An algorithm for incorporation of the adaptive reduction scheme into the reactive flow simulation is also presented in details.

5.1 Modeling reactive flows

Mathematical models describing the dynamics of reacting flows consist of systems of partial differential equations (PDEs), which specify advection, diffusion, and reaction of chemical species within a moving medium, and which couples the effects of non-reactive hydrodynamics with the effects of heat release in the chemical reactions. In the present study diffusion of chemical species and heat conduction and radiation effects are ignored, in order to keep the model simple. The aim of this work is to incorporate the adaptive reduction scheme in detailed flow models, and test its performance in detailed simulations. Using the proposed framework, if the adaptive scheme can be shown to perform accurately and efficiently in the detailed convection-reaction system then extending it to general Navier-Stokes equation will be straightforward, and will be considered in the future. The

advection-reaction system gives rise to the following conservative differential equation :

$$\frac{\partial \mathbf{u}}{\partial t} + \frac{\partial \mathbf{f}}{\partial x} + \frac{\partial \mathbf{g}}{\partial y} = \mathbf{S} \tag{5.1}$$

where $\mathbf{S}$ is the reaction source term and

$$\mathbf{u} = \begin{bmatrix} \rho \\ \rho \mathbf{V} \\ \rho e_T \\ \rho y_1 \\ \vdots \\ \rho y_{n_s} \end{bmatrix} = \text{vector of conserved quantities}$$

and

$$\mathbf{f} = \begin{bmatrix} \rho u \\ \rho u^2 + P \\ \rho uv \\ (\rho e_T + P)u \\ \rho u y_1 \\ \vdots \\ \rho u y_{n_s} \end{bmatrix}, \qquad \mathbf{g} = \begin{bmatrix} \rho v \\ \rho uv \\ \rho v^2 + P \\ (\rho e_T + P)v \\ \rho u y_1 \\ \vdots \\ \rho u y_{n_s} \end{bmatrix} \quad \mathbf{S} = \begin{bmatrix} 0 \\ 0 \\ 0 \\ 0 \\ \rho \omega_1 \\ \vdots \\ \rho \omega_{n_s} \end{bmatrix}$$

The characteristic time scales of chemical reactions are typically much shorter than the hydrodynamic time scales, which are determined by the local sound speed. Thus careful construction of numerical methods that accurately and efficiently handle the widely differing time scales and sharp gradients is of significant importance. Because of the disparity in time scales, the equations for the reactive gas dynamics model become stiff, with the reaction term much stiffer than the advection and diffusion terms. The method of lines (MOL) is a common approach towards the numerical integration of advection-diffusion-reaction equations, of which the reactive Navier-Stokes equations are a special case. This method first discretizes the equations in space, resulting in a large coupled system of ordinary differential equations (ODEs), which are then integrated in time. To avoid prohibitively small time steps imposed by the stiffness of the reaction terms in the ODEs, these terms can be integrated implicitly.

When applied to a system of ODEs obtained by MOL discretization, fully implicit methods treat every term implicitly and require the solution of implicit fully coupled

equations. In contrast, semi-implicit methods handle the advection term explicitly and integrate the diffusion and reaction terms implicitly. The non-linearity of the reaction terms makes the solution of such implicit equations computationally expensive, especially when the number of chemical species is large. Moreover, since the time step restricted by the stiff reaction terms has to be used for all processes, the computational cost of fully implicit or semi-implicit method can be significant.

Alternatively, an operator-splitting or time-splitting approach may be used. In this approach, the individual processes are decoupled and integrated sequentially, resulting in equations that are easier to solve. Moreover, by integrating slower processes using larger time steps, the overall computational cost can be reduced. The convective-reactive equation can be solved in two steps by first solving for the hydrodynamics and then solving for the reaction source term. The split equations are given by:

$$\frac{\partial \mathbf{u}}{\partial t} + \frac{\partial \mathbf{f}}{\partial x} + \frac{\partial \mathbf{g}}{\partial y} = 0 \tag{5.2}$$

$$\frac{\partial \mathbf{u}}{\partial t} = \mathbf{S} \tag{5.3}$$

Solution of the advective term of a conservation equation involves the solution of a Riemann problem, which can be computationally expensive. Thus the computational time can be substantially reduced by using a larger advection time step by decoupling it from the stiff reaction term. In the next step the ODEs consisting of the reaction terms are integrated, which will require much smaller time steps. However, in addition to the numerical errors arising in the integration of each term, the operator-splitting approach also introduces splitting errors, which reduce the accuracy of approximation. In the present study, the hydrodynamics was decoupled from the reaction using operator splitting approach. At each time step, the hydrodynamic portion is integrated using the Godunov scheme, and the reaction terms are integrated using the stiff ODE solver DVODE.

5.2 Riemann Problem

For any equation, such as the one-dimensional Euler equations or the scalar conservation equations, the *Riemann problem* has uniform initial conditions on an infinite spatial domain, except for a single jump discontinuity. For example, for the Euler equations, the

Riemann problem centered at $x = x_0$ and $t = t_0$ has the following initial conditions:

$$\mathbf{u}(x, t_0) = \begin{cases} \mathbf{u}_L, & x < x_0 \\ \mathbf{u}_R, & x > x_0 \end{cases}$$

where $\mathbf{u}_L, \mathbf{u}_R$ are constant vectors. The Riemann problem has an exact analytical solution for Euler equations, scalar conservation laws and any linear system of equations. Furthermore, the solution is *self-similar*, which means the solution stretches uniformly in space as time increases, but otherwise retains its shape. Hence $\mathbf{u}(x, t_1)$ and $\mathbf{u}(x, t_2)$ are similar to each other for any two times t_1 and t_2, since the solution depends on single variable x/t rather than on x and t independently. By reducing the number of independent variables, self-similarity simplifies solution techniques and sometimes even leads to analytical solutions, as in the case of the Riemann problem.

5.2.1 Riemann problem for Euler equations

The Riemann problem can be physically described by a one-dimensional tube containing two regions of stagnant fluid at different pressures, separated initially by a rigid diaphragm. If the diaphragm is instantaneously removed, the pressure imbalance causes a one-dimensional unsteady flow containing a steadily moving shock, a steadily moving simple centered expansion fan and a steadily moving contact discontinuity separating the shock and the expansion. This setup is referred to as the *shock tube*, as illustrated in Figure (). The flow in shock tube always has zero initial velocity. Removing this restriction, the shock tube problem becomes the Riemann problem. Like the shock tube problem, the Riemann problem problem may give rise to a shock, a simple centered expansion fan, and a contact separating the shock and expansion; however, unlike the shock tube problem, one or two of these waves may be absent. The exact solution of the Riemann problem can be analytically derived as:

- Solution for shock :

$$\frac{a_2^2}{a_1^2} = \frac{p_2}{p_1} \frac{\frac{\gamma+1}{\gamma-1} + \frac{p_2}{p_1}}{1 + \frac{\gamma+1}{\gamma-1}\frac{p_2}{p_1}}, \tag{5.4}$$

$$u_2 = u_1 + \frac{a_1}{\gamma} \frac{\frac{p_2}{p_1} - 1}{\sqrt{\frac{\gamma+1}{2\gamma}(\frac{p_2}{p_1} - 1) + 1}} \tag{5.5}$$

$$S = u_1 + a_1 \sqrt{\frac{\gamma+1}{2\gamma}(\frac{p_2}{p_1} - 1) + 1} \tag{5.6}$$

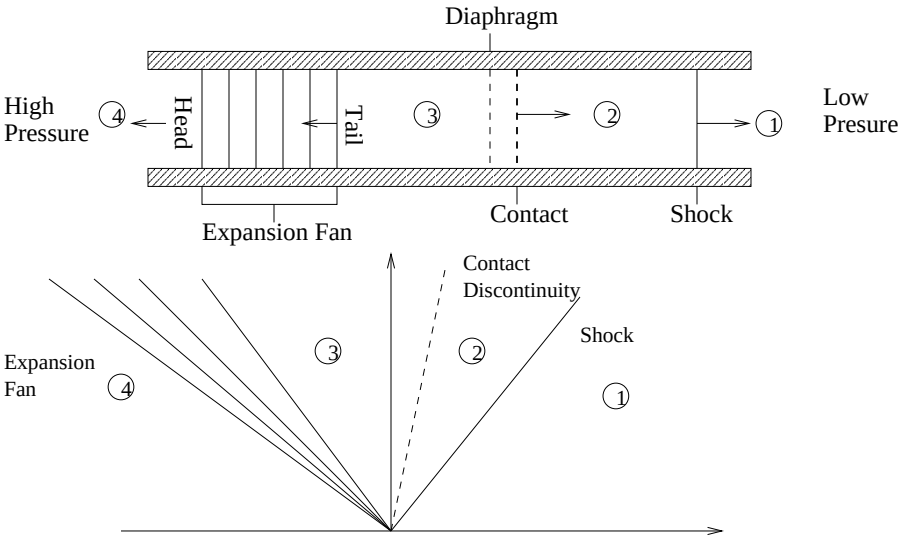

Figure 5.1: Performance of reduced mechanism with IEM as micromixing model

where S = speed of shock, a = speed of sound. u_1 and u_2 are the states to the right and left of the shock respectively.

- Contact discontinuity :

$$u_2 = u_3 \tag{5.7}$$

$$p_2 = p_3 \tag{5.8}$$

where u_2 and u_3 are the states to the right and the left of the contact, respectively.

- Simple centered expansion fan :

$$u(x,t) = \frac{2}{\gamma+1}\left(\frac{x}{t} + \frac{\gamma-1}{2}u_4 + a_4\right), \tag{5.9}$$

$$a(x,t) = u(x,t) - \frac{x}{t} = \frac{2}{\gamma+1}\left(\frac{x}{t} + \frac{\gamma-1}{2}u_4 + a_4\right) - \frac{x}{t}, \tag{5.10}$$

$$p = p_4\left(\frac{a}{a_4}\right)^{\frac{2\gamma}{(\gamma-1)}}. \tag{5.11}$$

Finally, the unknown pressure ratio across the shock $(\frac{p_2}{p_1})$ can be expressed in terms of the known pressure ratio $\left(\frac{p_4}{p_1}\right)$ as :

$$\frac{p_4}{p_1} = \frac{p_2}{p_1}\left(1 + \frac{\gamma-1}{2a_4}\left[u_4 - u_1 - \frac{a_1}{\gamma}\frac{\frac{p_2}{p_1}-1}{\sqrt{\frac{\gamma+1}{2\gamma}\left(\frac{p_2}{p_1}-1\right)+1}}\right]\right)^{\frac{-2\gamma}{\gamma-1}} \tag{5.12}$$

5.3 Numerical methods for Euler equations

The solution techniques for Euler equations can be broadly divided into two categories - flux approaches and wave approaches. Wave approaches can be further subdivided into two categories - flux vector splitting approaches and reconstruction-evolution approaches. Whereas flux approaches consider only fluxes, wave approaches model both fluxes and waves, and especially the interactions between various families of waves, using either flux vector splitting or Riemann solvers.

5.3.1 Flux approach

The flux approach of solving the Euler equation considers only flux, without making any effort to model waves. The commonly used flux approaches are the *Lax-Friedrichs method* and the *Lax-Wendroff method.*

Lax-Friedrichs method

The Lax-Friedrichs method for Euler equation is given by :

$$\mathbf{u}_i^{n+1} = \frac{1}{2}(\mathbf{u}_{i+1}^n + +\mathbf{u}_{i-1}^n) - \frac{\lambda}{2}(\mathbf{f}(\mathbf{u}_{i+1}^n) - \mathbf{f}(\mathbf{u}_{i-1}^n)) \tag{5.13}$$

Lax-Wendroff method

The Lax-Wendroff method for Euler equation is given by :

$$\mathbf{u}_i^{n+1} = \mathbf{u}_i^n - \frac{\lambda}{2}(\mathbf{f}(\mathbf{u}_{i+1}^n) - \mathbf{f}(\mathbf{u}_{i-1}^n)) + \frac{\lambda^2}{2}[A_{i+1/2}^n((\mathbf{f}(\mathbf{u}_{i+1}^n) - \mathbf{f}(\mathbf{u}_i^n)) - A_{i-1/2}^n((\mathbf{f}(\mathbf{u}_i^n) - \mathbf{f}(\mathbf{u}_{i-1}^n))]$$

5.3.2 Wave approach - Flux vector splitting

In this approach, the flux vector is written as :

$$\mathbf{f}(\mathbf{u}) = \mathbf{f}^+(\mathbf{u}) + \mathbf{f}^-(\mathbf{u}) \tag{5.15}$$

where the characteristic values of $d\mathbf{f}^+/d\mathbf{u}$ are all non-negative and the characteristic values of $d\mathbf{f}^-/d\mathbf{u}$ are all non-positive :

$$\frac{d\mathbf{f}^+}{\mathbf{u}} \geq 0, \frac{d\mathbf{f}^-}{\mathbf{u}} \leq 0 \tag{5.16}$$

The vector conservation law can then be written as :

$$\frac{\partial \mathbf{u}}{\partial t} + \frac{\partial \mathbf{f}^+}{\partial x} + \frac{\partial \mathbf{f}^-}{\partial x} = 0 \tag{5.17}$$

Then $\partial \mathbf{f}^+/\partial x$ can be discretized using FTBS (forward in time, backword in space) or some other equivalent methods, and $\partial \mathbf{f}^-/\partial x$ can be discretized using FTFS (forward in time, forward in space) or other similar methods. The resulting method will be completely stable for both left and right running waves.

To consider wave speed splitting, the flux jacobian matrix $A(\mathbf{u})$ is written as :

$$A(\mathbf{u}) = A^+(\mathbf{u}) + A^-(\mathbf{u}), \tag{5.18}$$

where the characteristic values of A^+ are non-negative and the characteristic values of A^- are non-positive.

$$A^+ \geq 0, A^- \leq 0 \tag{5.19}$$

The vector conservation law can be written as :

$$\frac{\partial \mathbf{u}}{\partial t} + A^+ \frac{\partial \mathbf{u}}{\partial x} + A^- \frac{\partial \mathbf{u}}{\partial x} = 0 \tag{5.20}$$

The matrices A^+ and A^- are obtained by splitting the characteristic values of A into positive and negative parts, which is called the wave speed splitting. In general the flux vector splitting and the wave speed splitting are distinct. However, the Euler equations have a special property that the flux vector is a homogenous function of order one, which implies that :

$$\mathbf{f}(\mathbf{u}) = \frac{d\mathbf{f}}{d\mathbf{u}}\mathbf{u} = A\mathbf{u} \tag{5.21}$$

This property makes the flux vector splitting and wave speed splitting essentially equivalent for the Euler equations. The commonly practiced flux vector splitting methods for Euler equations are the Stager-Warming method, Van Leer method, Liou-Steffen method, Zha-Bilgen method.

5.3.3 Wave approach - Reconstruction-Evolution

Spatial reconstruction

Finite difference methods use sample points as their primary representation, since it describes solutions in terms of rates of change at individual points. However, it needs to switch from samples to functional representations in order to differentiate or perform other functional operations. Any function created from sample points is called a *reconstruction.*

Temporal Evolution

In this step the solution is evolved from time level n to $n+1$ using characteristics or some other techniques. Hence for an approximate $u(x_{i+1/2}, t)$ for $t^n \leq t \leq t^{n+1}$:

$$\hat{f}^n_{i+1/2} = \frac{1}{\Delta t} \int_{t^n}^{t^{n+1}} f(u(x_{i+1/2}, t))dt \tag{5.22}$$

Any reasonable approximation based on waves and characeristics naturally introduces the minimal amount of upwinding required by the CFL condition.

Methods derived using this procedure are generally called *reconstruction- evolution* methods, a term coined by Harten, Engquist,Osher and Chakravarthy **?**. Alternatively they are sometimes called *Godunov-type method*, after the earliest such first-order accurate method. Reconstruction-evolution methods are extremely physical and elegant, though in practice it can be computationally expensive.

Godunov method

Godunov's method to obtain solution at $(n+1)\Delta t$ from solution at $n\Delta t$ involves 3 steps:

- Reconstruction : The reconstruction in this method is normally piecewise constant, as illustrated in Figure (5.2).

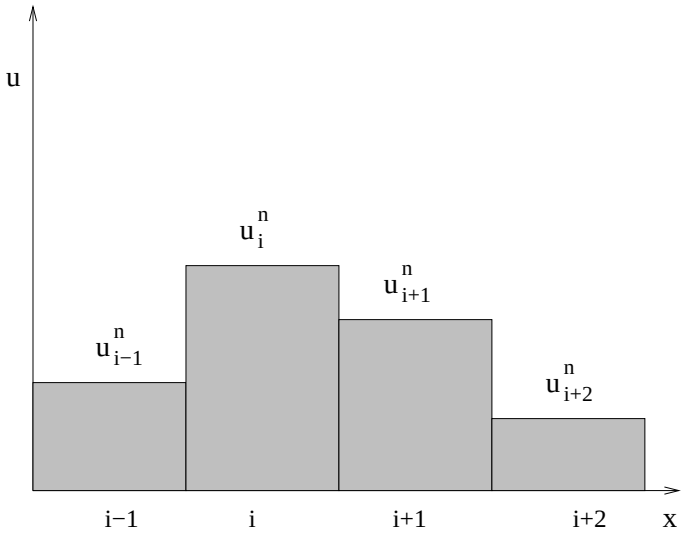

Figure 5.2: Piecewise constant reconstruction of each cell

- Evolution : Each cell edge gives rise to a local Riemann problem, as illustrated in Figure (5.3), which has to be solved at each cell interface $(i + 1/2)$. The original

Godunov method solves the Riemann problem exactly. Then the evolution of the piecewise- constant reconstruction yields

$$\hat{\mathbf{f}}^n_{i+1/2} = \frac{1}{\Delta t}\int_{t^n}^{t^{n+1}} \mathbf{f}(\mathbf{u}_{Riemann}(x_{i+1/2}, t))dt \tag{5.23}$$

Since the solution to the Riemann problem is self-similar, $\mathbf{u}_{Riemann}(x_{i+1/2}, t)$ is constant for all time. Hence

$$\hat{\mathbf{f}}^n_{i+1/2} = \mathbf{f}(\mathbf{u}_{Riemann}(x_{i+1/2}, t)) \tag{5.24}$$

where $\mathbf{u}_{Riemann}(x_{i+1/2}, t)$ is found using any exact or approximate Riemann solvers.

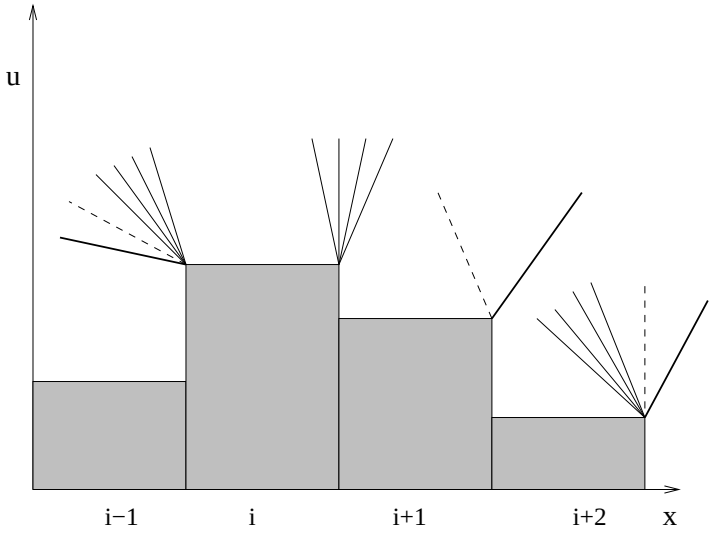

Figure 5.3: Each cell edge in a piecewise-constant reconstruction gives rise to a Riemann problem

- Projection : The state variables are averaged over each cell $[j-1/2, j+1/2]$ defining a new piecewise constant approximation at time step Δt.

The method described above is used to simulate the Riemann shock tube problem, for a single species, nonreactive case. The parameters used for the simulation are : $P_1 =$ 1 atm, $P_4 = 5$ atm, $\rho_1 = 0.0001\ gm/cm^3$, $\rho_4 = 0.0005 gm/cm^3$. Figure () illustrates the simulation results, and is observed that the Godunov method can accurately capture the behavior of the system, without giving rise to any spurious oscillations.

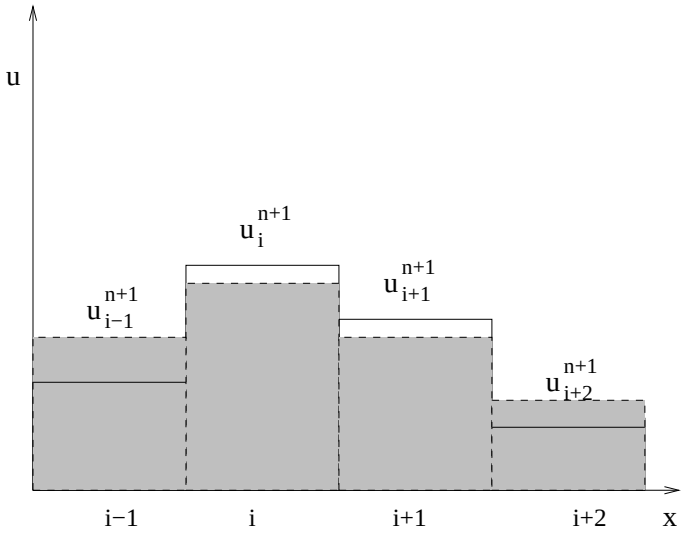

Figure 5.4: Projected solution at the next time step

To extend this method for the reactive flow simulation, the first step is to incorporate multiple species in the simulation. In the presence of single species, the conservation equations are solved for density, momentum and energy. In the presence of multiple species (N_s), additional conservation equations have to be satisfied for the $N_s - 1$ chemical species. The performance of the multi-species, nonreactive flow simulation is verified by again solving the shock tube problem. The pressure ratio considered is same as the previous simulation. The shock tube is assumed to be consisting of pure nytrogen at a temperature of 300K. Hence the density conditions are determined from the system property. Figure () illustrates the performance of the simulation.

The next step is the incorporation of reaction in the simulation. As described before, this is accomplished using the *operator splitting scheme*, where in each time step, the advection term is solved using the Godunov scheme, and the reaction source terms are integrated using a stiff ODE integrator. The overall PDE can be represented as:

$$\left.\begin{aligned} \mathbf{PDE} : \mathbf{u}_t + \mathbf{f}(\mathbf{u})_x = \mathbf{S}(\mathbf{u}) : 0 \leq x \leq L, \\ \mathbf{IC} : \mathbf{u}(x, t^n) = u^n \end{aligned}\right\}$$

Given the initial conditions, the soution has to be evolved from its initial value u^n at a time t^n, by one step of size Δt, to a value u^{n+1} at a time $t^{n+1} = t^n + \Delta t$. The spatial domain [0,L] is uniformly discretized into i grid points, following the finite difference approach. Hence u^n is a set of discrete values u_i^n at a time t^n. The discrete analog of the

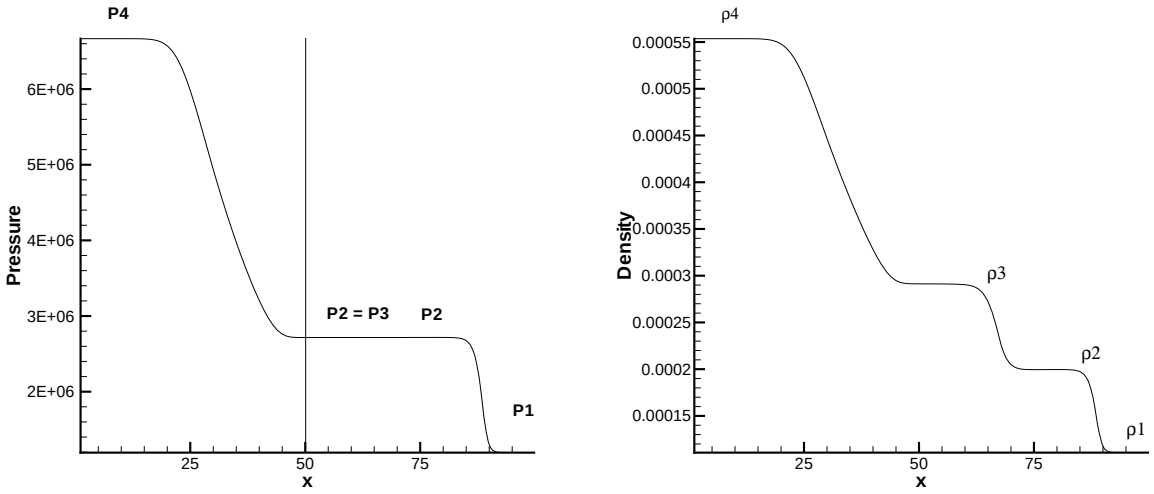

Figure 5.5: Simulation of Riemann shock tube problem using Godunov scheme

splitting scheme can then be represented as:

$$\left.\begin{array}{c}\mathbf{PDE}: \mathbf{u}_t + \mathbf{f}(\mathbf{u})_x = 0, \\ \mathbf{IC}: \mathbf{u}(x, t^n) = \mathbf{u}^n\end{array}\right\} \Longrightarrow \hat{\mathbf{u}}^{n+1} \quad \left.\begin{array}{c}\mathbf{ODE}: \frac{d}{dt}\mathbf{u} = \mathbf{S}(\mathbf{u}) \\ \mathbf{IC}: \hat{\mathbf{u}}^{n+1}\end{array}\right\} \Longrightarrow \mathbf{u}^{n+1}$$

The initial condition for the advection problem is the initial condition for the complete problem. The time step Δt is determined using the stability constraint of the advection problem, using CFL condition. The solution of the advection problem after a time Δt is denoted by $\hat{\mathbf{u}}^{n+1}$, and is used as the initial condition for the second initial value problem. This second problem accounts for the source term $\mathbf{S}(\mathbf{u})$, and is also solved for a complete time step Δt, however, the integrator for the stiff ODE allows for internal subcycling of timestep. This solution is regarded as the approximation to the solution $\mathbf{u}^{n+1}$ of the full problem at a time t^{n+1}. This splitting scheme is first order accurate, and it is possible to increase the order of aacuracy by using more complex splitting schemes.

5.3.4 Coflow nonpremixed methane-air flame

The unconfined, co-flow non-premixed methane/air flame is chosen to illustrate the performance of the developed adaptive chemistry scheme. The burner consists of two concentric tubes as illustrated in Figure (5.7). A stream of methane is injected through the inner tube, surrounded by a stream of air, injected through the outer tube. A cylindrical chimney confines the flame. Many computational and experimental studies have been carried

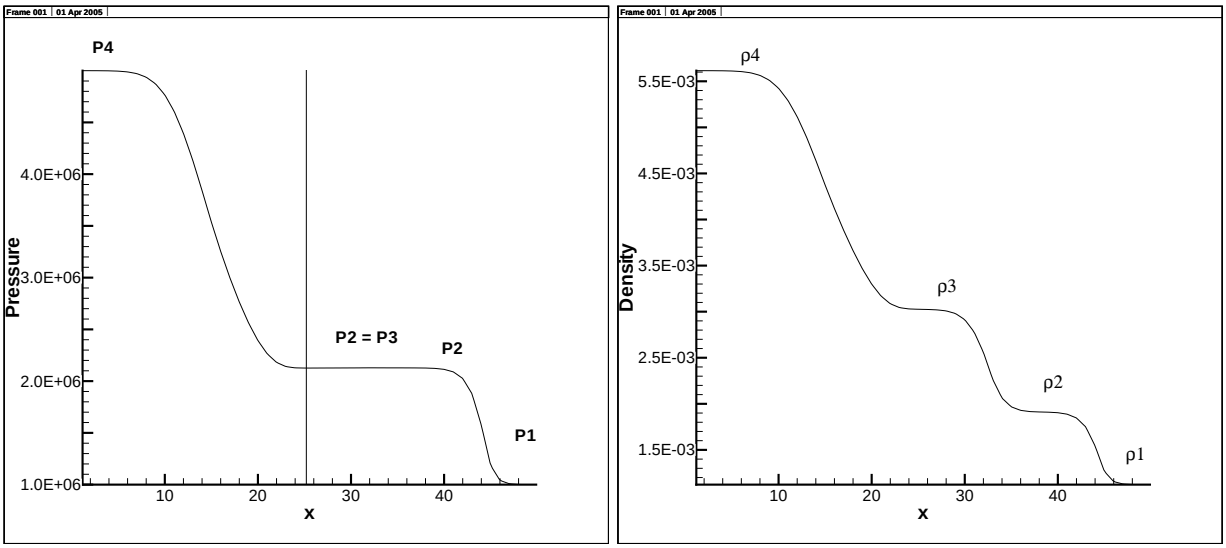

Figure 5.6: Simulation of Riemann shock tube problem using Godunov scheme, with multiple species

out for these flames in different physical configurations /cite.

The geometrical parameters used for the present problem are : inner radius $r_i = 0.2cm$, outer radius $r_o = 2.5cm$, chimney height $L = 5cm$. At the inlet, the temperature is 300K and the fuel velocity is $u = 0, v = 20cm/s$. The inlet air velocity is $u = 0, v = 25cm/s$. The flame is ignited by a hot patch (T = 1500K) next to the inlet. A grid size of 50×50 is used to cover the 5 cm $\times$ 5 cm computational domain. Simulations are performed using both detailed kinetic model and the proposed adaptive scheme, to verify and validate the performance of the adaptive scheme in detailed reactive flow models.

5.4 Incorporation of adaptive chemistry in flow model

In the previous section the reactive flow model uses the same chemistry model throughout the entire simulation. Hence the number and description of chemical species remains unchanged for the whole simulation. The idea behind the adaptive scheme, however, is to change the chemistry model with time and space, depending on the local species and temperature conditions. The generation of multiple reduced model and construction of the library of reduced model was discussed in Chapter (4). The feasibility analysis of individual reduced model was performed following the technique presented in Chapter (3), and stored in the library corresponding to the reduced model. These simulations were

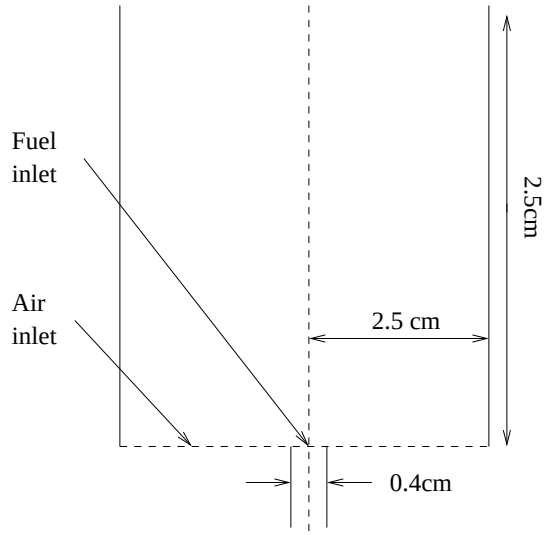

Figure 5.7: Schematic of the specifications of co-flow methane-air flame

performed *apriori* and the complete library was constructed before starting the detailed reactive flow simulation. The incorporation of the adaptive chemistry scheme in the reactive flow model requires some minor modification of the model equations. First, the flow model has to be written for all the species present in the detailed chemistry model, hence at all time the system will retain all the chemical species. This is to enable the simulation to change from one reduced model to another without violating species and mass conservation, since two reduced model can contain different species. The conservative equations are written by modifying the source term as:

$$\mathbf{S}_{mod} = \begin{bmatrix} 0 \\ 0 \\ 0 \\ 0 \\ \lambda_1 \rho\omega_1 \\ \lambda_2 \rho\omega_2 \\ \vdots \\ \lambda_{n_s} \rho\omega_{n_s} \end{bmatrix}$$

where $\lambda_1, \lambda_2, \ldots, \lambda_{n_s}$ are a particular combination of binary variables representing a unique reduced model. For example, if all the λs are zero, then the entire source term becomes zero, implying no-rxn condition. On the other hand, if all the λs are 1, then all the

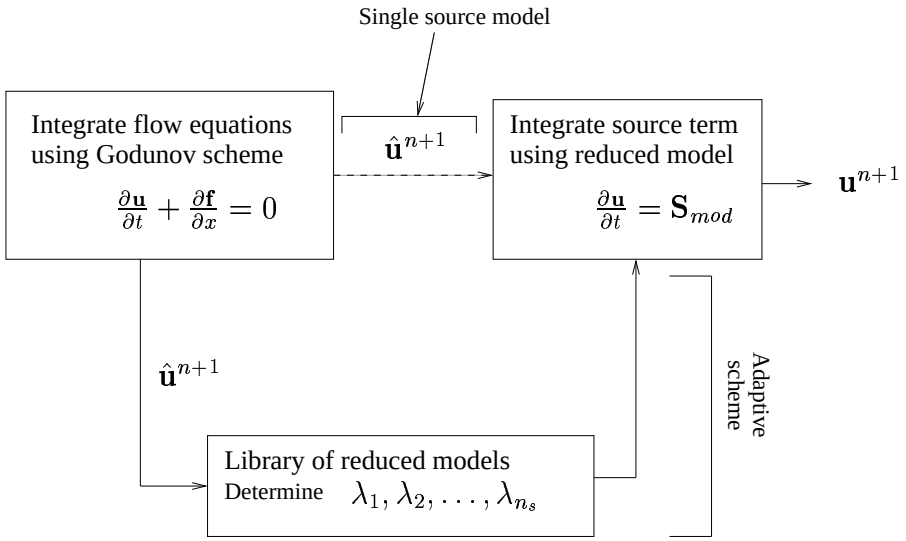

Figure 5.8: Integration of the adaptive scheme with flow simulation

species will be integrated in the reaction step, implying the use of the detailed chemistry model. These two are the extreme cases, any other combination of λ will specify a reduced chemistry model. In the context of operator splitting approach, this implies that at every time step, the flow model will be integrated for all the 53 species of the detailed methane chemistry (GRI-3.0). At the end of flow integration, and before starting the reaction step, the appropriate reduced chemistry model needs to be determined from the library of reduced model. This is accomplished by passing the conditions obtained at the end of the flow step to the pre-constructed library, and checking the feasible region of the stored reduced models by the point-in-polygon algorithm to find a model which is feasible under present conditions. The chosen reduced model is specified by a particular combination of λ, using which the source term is reconstructed and integrated. This integration of the adaptive chemistry scheme with the flow simulation is illustrated in Figure (5.8).

5.5 Summary

The development of a detailed reactive flow model is discussed in this chapter, along with the integration of the adaptive chemistry scheme with the flow model. The operator splitting scheme is used to decouple the flow equations from the reaction source term, since it enables the use of different optimized methods for integration of individual terms. In

the absence of diffusion and heat conduction, the flow equation reduces to Euler equation, consisting of multiple species, which is integrated using the Godunov scheme. The reaction term is integrated using stiff ODE solver, DVODE, which allows subcycling of time steps. The subcycling of reaction time step guarantees solution convergence, without restricting the time step requirement of the flow step. The splitting scheme used in the present work is first order, hence the whole scheme will be first-order accurate, even if individual integration schemes are of higher order. However, it is possible to increase the accuracy of the scheme by using Strang splitting or other higher order splitting schemes.

A scheme is presented to integrate the adaptive chemistry with the flow simulation, in the context of split-timestep approach, where, before performing the reaction integration, an appropriate reduced model is selected and integrated, thereby saving the computational work load. However, the use of the proposed adaptive scheme is not restricted to the split timestep approach, and can be generalized to any other integration scheme.

Chapter 6

Summary and future directions

In this thesis, a novel adaptive chemistry scheme is presented which enables accurate simulation of reactive flow systems, which are otherwise computationally demanding. The conventional approach to deal with such expensive computations is to approximate the complex kinetic mechanism by a simple reaction model. Such simulations, though helpful in providing an insight to the simulated system, fail to capture the detailed behavior of the system in the absence of the detailed chemistry representation. The present work bridges this gap by developing the adaptive chemistry scheme, where multiple reduced models are developed and characterized by their range of validity. This enables the reactive flow simulation to retain both accuracy and computational feasibility, by always using a locally-accurate reduced chemistry model. The presented scheme is found to have satisfactory performance, as illustrate by the example problems. However, it is possible to further improve its performance, as will be discussed in this chapter.

6.1 Mechanism reduction

6.1.1 Application to very large mechanisms

In this work, the kinetic mechanism reduction problem is formulated as a mathematical programming problem, and generation of a reduced model requires solution of an integer programming problem. This scheme indeed gives rise to accurate and flexible reduced models, but is itself an expensive operation since it requires multiple integration of the stiff, nonlinear ODEs describing the kinetic source term. Also, the number of binary

variables handled by the MINLP formulation can be restrictive. Thus direct application of this procedure in reduction of very large mechanisms, consisting of thousands of chemical species may prove to be inefficient. For such cases, it may be efficient to use a bi-level reduction procedure, where a first level reduction can be performed using less expensive methodologies based of flux-analysis **?**, followed by the more detailed reduction using the integer programming approach.

6.1.2 Development of reduced models with specific characteristics

The mechanism reduction procedure outlined in chapter 2 results in simplified kinetic models which can predict the profiles of specific species within specified tolerance. However, in many of the combustion problems, what is of more importance is not just specific species conentration, but certain specific combustion characteristics, which also provides stringent test beds for the detailed as well as reduced kinetic schemes. Those include :

Shock-tubes

The shock tube experiments are an excellent test of high temperature reaction mechanism for hydrocarbon oxidation. The most common observable quantity in such systems is the ignition delay time, generally defined as the time at which noticeable heat release or pressure rise is observed in the reacting gases.

Flow reactors

The turbulent flow reactors provide an environment complimentary to that of shock-tube. Here the temperatures are considerably lower than that of shock tube. The initiation reaction plays virtually no role in the flow reactors, but the period of fuel comsumption and production of stable intermediates is easily accessible.

Flame propagation

Laminar flames are among the earliest combustion problems to be studied theoretically that required simultaneous consideration of both fluid dynamics and chemical kinetics for its solution (Kailashnath (1991)). There has been numerous analytical and computational studies of various flame related phenomena like flame ignition, flame quenching, flame propagation velocities, flammability limits, flame instabilities, etc.

Generation of reduced kinetic models which can predict those combustion character-

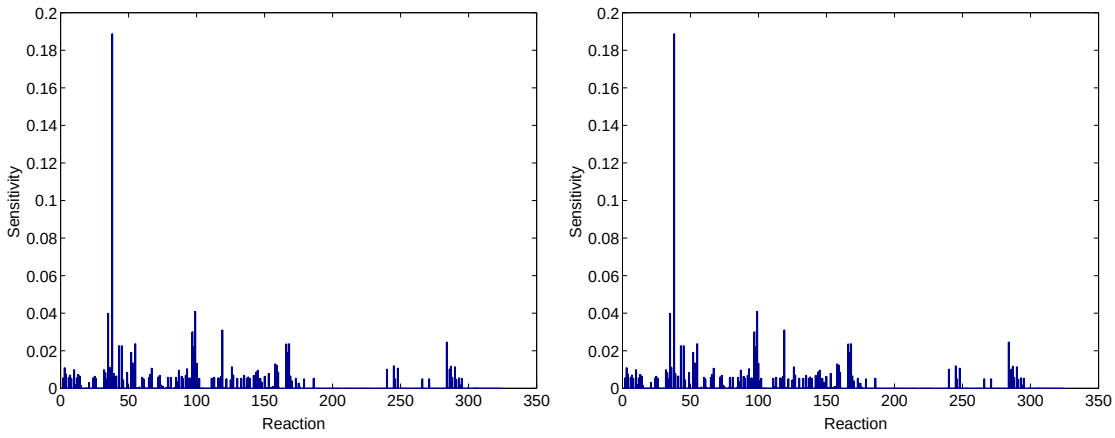

Figure 6.1: Sensitivity of laminar flame speed to individual species and reaction

istics with high accuracy is of great importance. The proposed approach of mechanism reduction has great flexibility of generating a reduced mechanism which can predict profiles of specific species with desired accuracy. However, it is possible that the specified species does not contribute significantly towards the desired combustion characteristic. For example a simplified model of GRI-3.0 obtained considering CH_4, H_2, O_2 and T in the error estimate was used to test the laminar flame speed prediction, which was found to perform poorly with 52% deviation from the actual value. Hence in order to generate reduced mechanism which can accurately predict specific characteristics, the species sensitivities to this specific characteristic is first evaluated. Considering flame speed, the results of the sensitivity analysis for GRI-3.0 mechanism performed with respect to individual species and reaction is shown in Figure(6.1.2), where it is observed that O and H are the species with higher sensitivity. All the other species resulted in less than 10% change of flame speed. The reduction was then performed considering O,H and T in the error function with a high tolerance limit in order to result in good prediction of the profiles. The obtained reduced set consists of 18 species and 33 reactions, and predicts the flame speed within 12% of the actual value. Present work is directed towards further improvement of the prediction of the main combustion characteristics by incorporating the calculation of the flame speed at the intermediate stages of the reduction algorithm, guiding the approach towards accurate flame speed prediction.

Species	% change in flame speed
H_2	37
H	81
O	93
C	33

Table 6.1: Flame speed sensitivity analysis of GRI-3.0

6.2 Feasibility analysis

Accurate analysis of the range of validity of the reduced chemistry models is of utmost importance for the success of the proposed scheme. The feasibility analysis scheme presented in chapter 3 is based on surface reconstruction ideas, where the range of validity of the reduced model is first sampled, and the sampled points are given a mathematical description. This scheme is extremely successful in capturing arbitrary shaped feasible region, which is the case in the present problem. The primary limitation of this technique is that it is efficient in low dimension, and its extension to higher dimension is computationally challenging. In the presented problem, the reduced models were checked for its feasibility in a 3-dimensional state space of CH_4 and O_2 concentration and temperature. For all the problems handled this far using methane combustion, it is observed that feasibility in this 3-dimensional space is sufficient to capture the accurate behavior of the reduced models even in the presence of additional species. However, this may not be true for more complex fuels and it may prove to be useful to extend this procedure to higher dimensions. One way of dealing with this issue is by reducing the dimensionality of the problem. The ideas of principal component analysis Vajda et al. (1985) can be utilized to map the original uncertainty space to the reduced dimensional space of important eigen directions. The α shape ideas can then be applied in the reduced space and the feasibility information mapped back to the original uncertain space.

6.3 Adaptive chemistry scheme

The adaptive chemistry scheme presented in chapter 4 enables the flow simulation to choose an appropriate reduced model from the library of precompiled reduced models.

The success of this scheme in saving the computational workload largely depends on the developed library, since in the absence of a locally accurate reduced model the simulation will have to integrate the detailed model. While it is not difficult to generate a more complete library of reduced models addressing widely diverse conditions in the state space, but scanning the entire library to determine the accurate model can become a restrictive operation. For the present simulation the library consists of 20 reduced models, for which the search is not demanding, but it can become so for a much larger library. In the present scheme, reduced models are arranged in the library in an ascending order of their species numbers, and at every step the simulation searches in a top down direction, starting from the simplest towards progressively complex models. This search can be made more efficient by storing information about the connectivity or proximity of the individual reduced models, accompanied by the memory of previously chosen reduced model at each point. While selecting a reduced model the simulation will first check the previous selection for its validity. If this is not valid, then it will look at the neighboring models to find an appropriate one, and so on. This is likely to reduce the search time, based on the understanding that the conditions in a grid changes gradually with time. Given the small time steps required for convergence, it is unlikely that the conditions will change so drastically to end up in a different domain of the state space.

6.4 Integration with flow simulation

In chapter 5, a detailed reactive flow model was developed based on the operator splitting scheme, where the flow equations are integrated using Godunov scheme and the source terms are integrated using DVODE. In order to implement the adaptive chemistry model in the flow simulation, the first step is to develop a multi-species reactive flow code, where all the species present in the detail chemistry model needs to be present. The approach used in this work is that the flow equations will be integrated for all the species, but the reaction source term will be integrated only for the reduced species. While integration of the reduced chemistry model will reduce the computational workload, but integration of the flow model using all the species may increase the workload for certain applications. However, it is essential to retain all the chemical species in the system to conserve mass. One approach to handle this problem can be to retain all the species, but to divide them

into *active* and *passive* groups based on the species concentration, or some other relevent criterion. The convective velocity can then be computed using only the active species, assuming that the passive species will have negligible contribution to this velocity. The passive species will then be convected using the same velocity determined by the active species. This approach is likely to reduce the computational cost of the multispecies flow integration. However, the exact details will largely depend on the particular integration scheme used.

The example presented in chapter 5 integrates the Euler equation, where species diffusion and heat conduction are neglected. While this model provides a good test bed to validate the adaptive scheme, but is not justified in modeling a subsonic reactive flow simulation like deflagration. Such assumptions hold good for detonation simulations, where molecular phenomenon like diffusion and conduction have negligible effect. Extension of present work to detonation simulation will require development of reduced models under high pressure conditions. The other possible extension is to incorporate the diffusion and conduction effects and solve the Navier-Stokes equation for flame propagation.

This thesis successfully validates the use of adaptive chemistry scheme in reactive flow simulations, but the main success of a model is in its predictive capacity, where it can either predict conditions to help guide the experimental work, or capture phenomenon which cannot be observed experimentally. Towards this end, the future direction of the presented work is to include diffusion, conduction, along with Dufor and Soret effects, which are known to influence deflagration process.

Bibliography

Akl, S., Toussaint, G., 1978. Efficient convex hull algorithm for pattern recognition applications. *Proc. Fourth Int. Jr. Conf. Pattern Recognition* , 483.

Androulakis, I. P., 2000. Kinetic mechanism reduction based on an integer programming approach. *AIChE J.* 46, 361.

Balakrishnan, S., Georgopoulos, P., Banerjee, I., Ierapetritou, M., 2002. Uncertainty considerations for describing complex reaction systems. *AIChE J.* 48, 2875.

Barber, C. B., Dobkin, D., Huhdanpaa, H., 1996. The quickhull algorithm for convex hulls. *Comp. and Chem. Eng.* 22, 469.

Bard, Y., 1974. *Nonlinear parameter estimation.* Academic, New York.

Berg, M., van Kreveld, M., Overmars, M., Schwarzkopf, O., 1997. *Computational geometry: Algorithms and applications.* Sprieger.

Borghi, R., 1988. Turbulent combustion modelling. *Prog. Energy Combust. Sci.* 14, 245.

Box, G., Draper, N., 1987. *Empirical model-building and response surfaces.* Wiley, New York.

Chen, J. Y., 1997. Stochastic modeling of partially stirred reactors. *Combust. Sci. and Tech.* 122, 63.

Correa, S. M., 1993. Turbulence-chemistry interactions in the intermediate regime of premixed combustion. *Combust. and Flame* 93, 41.

Curl, R. L., 1963. Dispersion phase mixing. i theory and effects in simple reactor. *AIChE J.* 9, 175.

DeJong, K., 1975. *An analysis of the behavior of a class of genetic adaptive systems.* Doctoral dissertation, University of Michigan, Ann Arbor, Michigan.

Edelsbrunner, H., 1992. Weighted alpha shapes. *Tech. Rep. UIUCDCS-R-92-1760*, Dept. of Comp. Sc., UIUC,IL .

Edelsbrunner, H., Kirkpatrick, D., Seidel, R., 1983. On the shape of a set of points in a plane. *IEEE Trans. Inform. Theory IT-29* , 551.

Edwards, K., Edgar, T., Manousiouthakis, V. I., 1998. Kinetic model reduction using genetic algorithm. *Comp. and Chem. Eng.* 22, 239.

Edwards, K., Edgar, T. F., Manousiouthakis, V. I., 2000. Reaction mechanism simplification using mixed-integer nonlinear programming. *Comp. and Chem. Eng.* 24, 67.

Ester, M., Kriegel, H., Sander, J., Xu, X., 1996. *A density based algorithm for discovering clusters in large spatial database with noise* . Intl. conference on knowledge discovery in databases and data mining, Montreal, Canada.

Ester, M., Kriegel, H., Xu, X., 1993. *A database interface for clustering in large spatial databases* . Intl. conference on knowledge discovery in databases and data mining, Montreal, Canada.

Fairfield, J., 1979. Contoured shape generation forms that people see in dot patterns. *Proc. IEEE Conf. Cybernet and Soc.* , 60.

Frenklach, M., 1984. *Modeling, Combustion chemistry, edited by W.C. Gardiner.* Springer-Verlag, New York.

Glassman, I., 1996. *Combustion.* Academic Press.

Goldberg, D. E., 1989. *Genetic algorithms in search, optimization and machine learning.* Addison-Wesley, New York.

Goyal, V., Ierapetritou, M., 2002. Determination of operability limits using simplicial approximation. *AIChE J.* 48, 2902.

Guha, S., Rastogi, R., Shim, K., 1998. Cure: An efficient clustering algorithm for large databases. *Proc. ACM SIGMOD* , 73.

Haines, E., 1994. Point in polygon strategies. *Graphic Gems* ed.Paul Heckbert, Academic Press , 24.

Halemane, K., Grossmann, I., 1983. Optimal process design under uncertainty. *AIChE J.* 29, 425.

Hindmarsh, A. C., 1983. ODEPACK, A systematized collection of ODE solvers. Scientific Computing, Stepleman, R.S. *et al.* (eds.), North Holland, Amsterdam.

Jarvis, R., 1977. Computing the shape hull of points in the plane. *Proc. IEEE Comp. Soc. Conf. Pattern Recognition and Image Processes* , 231.

Kailashnath, K., 1991. *Laminar flames in premixed gases.* Numerical approaches to combustion modeling, Edited by Oran, E.S., Boris, J.P.

Kee, R., Rupley, F., Meeks, E., Miller, J. A., 1996. CHEMKIN-III: A Fortran chemical kinetics package for the analysis of gas-phase chemical and plasma kinetics. Sandia report, m SAND96-8216.

Kirkpatrick, D., Radke, J., 1985. A framework for computational morphology. *Computational Geometry*, Elsevier North Holland, NY , 234.

Kuo, J., Wei, J., 1969. A lumping analysis in monomolecular reaction systems. analysis of approximately lumpable systems. *Ind. Engg. Chem. Fund.* 8, 124.

Lam, S. H., Goussis, D. A., 1994. The csp method for simplifying chemical kinetics. *Int. J. Chem. Kinet.* 26, 461.

Mandal, D., Murthy, C., 1997. Selection of alpha for alpha-hull in $\mathscr{R}^2$. *Pattern Recognition* 30, 1759.

Mass, U., Pope, S. B., 1992. Simplifying chemical kinetics: Intrinsic low dimensional manifold in composition space. *Combust. and Flame* 88, 239.

Matula, D., Sokal, R., 1980. Properties of gabriel graphs relevant to geographic variation research and the clustering of points in the plane. *Geograph. Anal.* 12, 205.

Michalewicz, Z., Schoenauer, M., 1996. Evolutionary algorithms for constrained parameter optimization problems. *Evol. Comput.* 4, 1.

Peters, N., 1988. Systematic reduction of flame kinetics : Principles and details. *Prog. Astronaut. Aeronaut.* 113, 67.

Petzold, L., Zu, W., 1997. Model reduction for chemical kinetics: An optimization approach. *AIChE meeting*, Los Angeles.

Pope, S. B., 1985. Pdf methods for turbulent reactive flows. *Prog. Energy Combust. Sci.* 11, 119.

Pope, S. B., 1997. Computationally efficient implementation of combustion chemistry using *in situ* adaptive tabulation. *Combust. Theory Model.* 1, 41.

Raymond, T., Han, J., 1994. *Efficient and effective clustering methods for spatial data mining.* Proc. of the VLDB conference, Santiago, Chile.

Sirdeshpande, A. R., Ierapetritou, M. G., Androulakis, I. P., 2001. Design of flexible reduced kinetic mechanism. *AIChE J.* 11, 2461.

Swaney, R., Grossmann, I., 1985. An index for operational flexibility in chemical process design i: Formulation and theory. *AIChE J.* 31, 621.

Tomlin, A. S., Turanyi, T., Pilling, M. J., 1997. Mathematical methods for the construction, investigation and reduction of combustion mechanisms. *Low-temperature combustion and auto ignition*, M.J. Pilling, ed., Chemical Kinetics, 35.

Toussaint, G., 1980. The relative neighborhood graph of a finite planar set. *Pattern Recognition* 12, 261.

Turanyi, T., Hughes, K., Pilling, M., Tomlin, A., 1996. KINALC: Program for the analysis of reaction mechanisms. *Combustion simulations at the University of Leeds.*

Vajda, S., Valko, P., Turanyi, T., 1985. Principal component analysis of kinetic models. *Int. J. Chem. Kinet.* 17, 55.

Wei, J., Kuo, J., 1969. A lumping analysis in monomolecular reaction systems. analysis of exactly lumpable systems. *Ind. Engg. Chem. Fund.* 8, 114.

Williams, F. A., 1985. *Combustion theory.* Benjamin cummings, Menlo park, CA.

Zhang, T., Ramkrishnan, R., Livny, M., 1996. *BIRCH : An efficient data clustering method for very large data bases*. Proc. of the ACM SIGMOD conf. on management of data, Montreal, Canada.